Electronic Supplementary Material (ESI) for Chemical Science

Self-Assembly of Bicyclic Dinuclear *tris*-(Ditopic Diphosphane) Complexes of Zerovalent Group 10 Metals

Daniel Tofan

Christopher C. Cummins*

Department of Chemistry, Massachusetts Institute of Technology, Cambridge MA 02139-4307

E-mail: ccummins@mit.edu

May 2, 2012

*To whom correspondence should be addressed

Table of Contents

S.1 Synthetic and Spectroscopic Details

S.1.1 General Procedures

All manipulations were performed in a Vacuum Atmospheres model MO-40M glove box under an inert atmosphere of purified N_2. Solvents were obtained anhydrous and oxygen-free by bubble degassing (N_2) and purification using a Glass Contours Solvent Purification System built by SG Water. Deuterated solvents were purchased from Cambridge Isotope Laboratories, degassed, and stored over molecular sieves prior to use. All glassware was oven-dried at temperatures greater than 170 °C prior to use. Celite 435 (EM Science) was dried by heating above 200 °C under a dynamic vacuum for at least 48 h prior to use, while alumina (activated, basic, Brockman I) was dried similarly for at least 7 days prior to use. ^{1}H, ^{13}C and ^{31}P NMR spectra were obtained on Varian Mercury 300, Varian Inova 500, or Bruker Avance 400 instruments equipped with Oxford Instruments superconducting magnets, and were referenced to appropriate solvent resonances.[1] ^{31}P NMR spectra were referenced externally to 85% H_3PO_4 (0 ppm). Elemental analyses were performed by Midwest Microlab LLC, Indianapolis, IN. White phosphorus was acquired from Thermphos International, while all other reagents were purchased from commercial sources.

S.1.2 Synthesis of Complex (η^1-**1**)Ni(μ-**1**)$_3$Ni(η^1-**1**) (**2**)

A solution of **1** (102 mg, 0.45 mmol, 5.0 equiv) in THF (5 mL) was added to a THF (4 mL) solution of Ni(cod)$_2$ (50 mg, 0.18 mmol, 2.0 equiv) under stirring. The mixture turned immediately from yellow to orange, and then to dark brown. After 15 min, all volatile materials were removed under reduced pressure and the remaining residue was redissolved in THF (3 mL). The mixture was stored at –35 °C and the precipitate that formed was collected via suction filtration on a fritted glass filter, washed with cold pentane, and dried under reduced pressure to yield bright yellow solids containing analytically pure complex **2** (54 mg, 0.043 mmol, 48% yield). ^{1}H NMR (C_6D_6, 20 °C, 400 MHz) δ: 2.75–2.70 (m, 4 H, $^{\eta^1}CH_2$), 2.69 (d, $^{2}J_{HH}$ = 14.4 Hz, 12 H, $^{\mu}CHH$), 2.53 (d, 12 H, $^{\mu}CHH$), 2.33–2.17 (m, 12 H, $^{\eta^1}CH_2$), 1.90 (s, 12 H, $^{\eta^1}CH_3$), 1.81 (s, 36 H, $^{\mu}CH_3$), 1.77 (s, 12 H, $^{\eta^1}CH_3$) ppm (Figure S.1); assignments were made based on the ^{1}H–^{1}H COSY NMR spectrum (Figure S.2). ^{13}C{^{1}H} NMR (C_6D_6, 20 °C, 100.6 MHz) δ: 126.5 ($^{\eta^1}CH_0$), 126.3 ($^{\mu}CH_0$), 125.1 (d, $^{2}J_{CP}$ = 7 Hz, $^{\eta^1}CH_0$), 40.6 ($^{\mu}CH_2$), 40.1 ($^{\eta^1}CH_2$), 28.5 ($^{1}J_{CP}$ = 34.0 Hz, $^{\eta^1}CH_2$), 23.4 ($^{\mu}CH_3$), 23.2 ($^{\eta^1}CH_3$), 22.0 ($^{\eta^1}CH_3$) ppm (Figure S.3). ^{31}P{^{1}H} NMR (C_6D_6, 20 °C, 121.5 MHz) δ: –7.3 (d-vsept, $^{1}J_{PP}$ = 344 Hz, 2 P, NiP_AP$_M$), –30.2 (vt-vt, $^{2+3}J_{PP}$ = 55.9 Hz, $^{3+4}J_{PP}$ = 22.1 Hz, 6 P, Ni$P_X P_X$Ni), –62.1 (d-vsept, 2 P, NiP$_A P_M$) ppm (Figure S.4). Elemental analysis [%] found (and calcd. for $C_{60}H_{100}Ni_2P_{10}$): C 58.03 (57.72); H 7.85 (8.07); N none (0.00); P 24.46 (24.81).

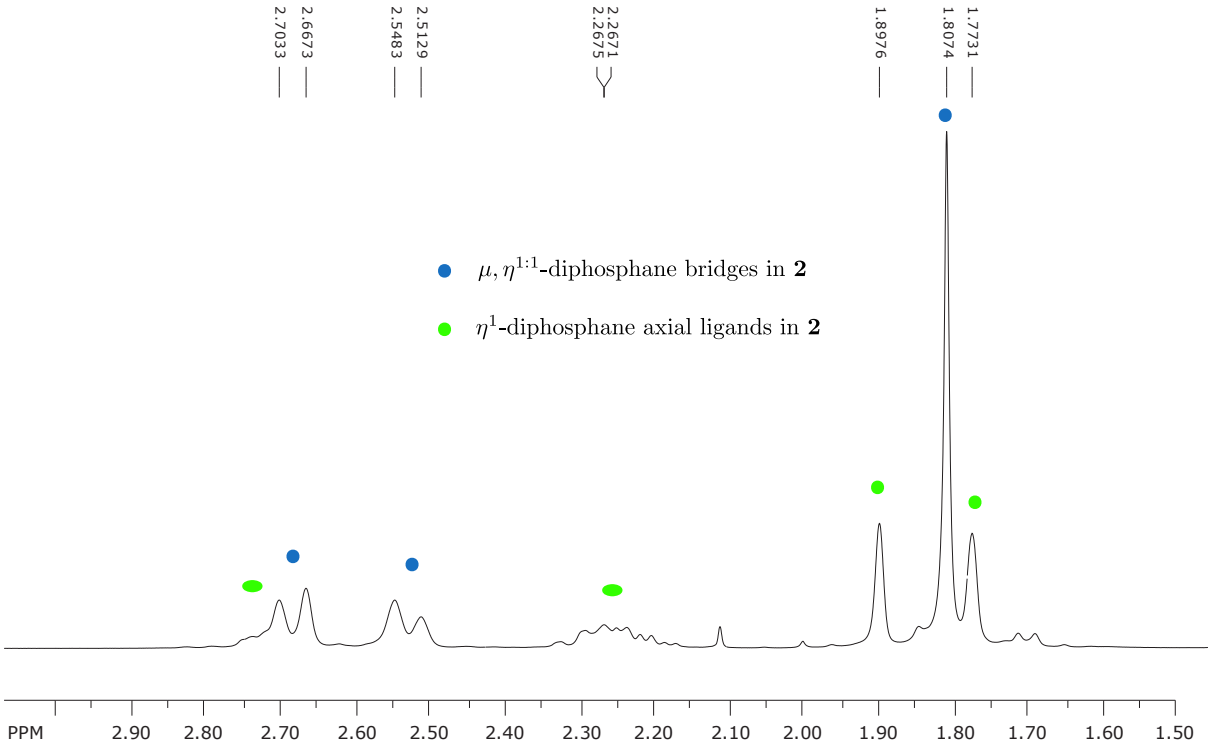

Figure S.1: ^{1}H NMR spectrum of complex **2**.

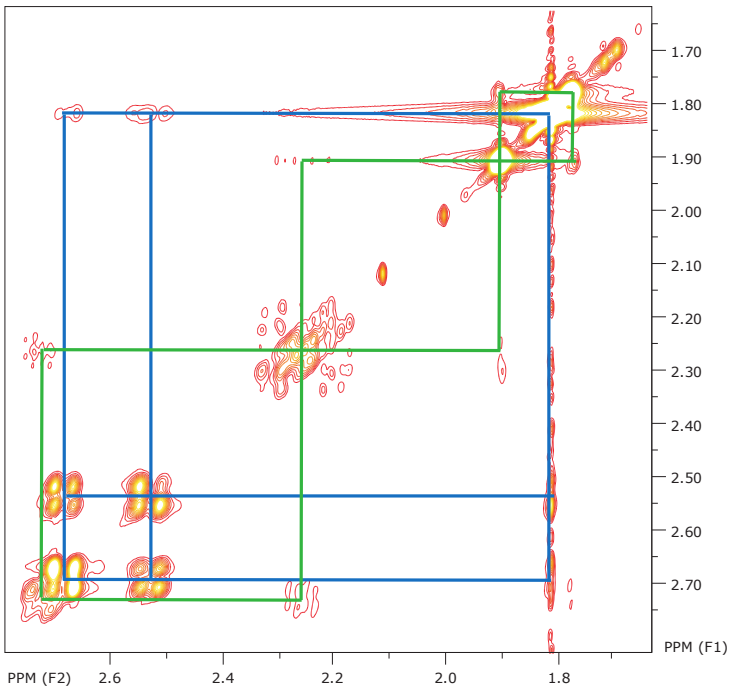

Figure S.2: ^{1}H-^{1}H COSY spectrum of complex **2** with separate coupling patterns at bridging (blue) and terminal (green) diphosphane ligands.

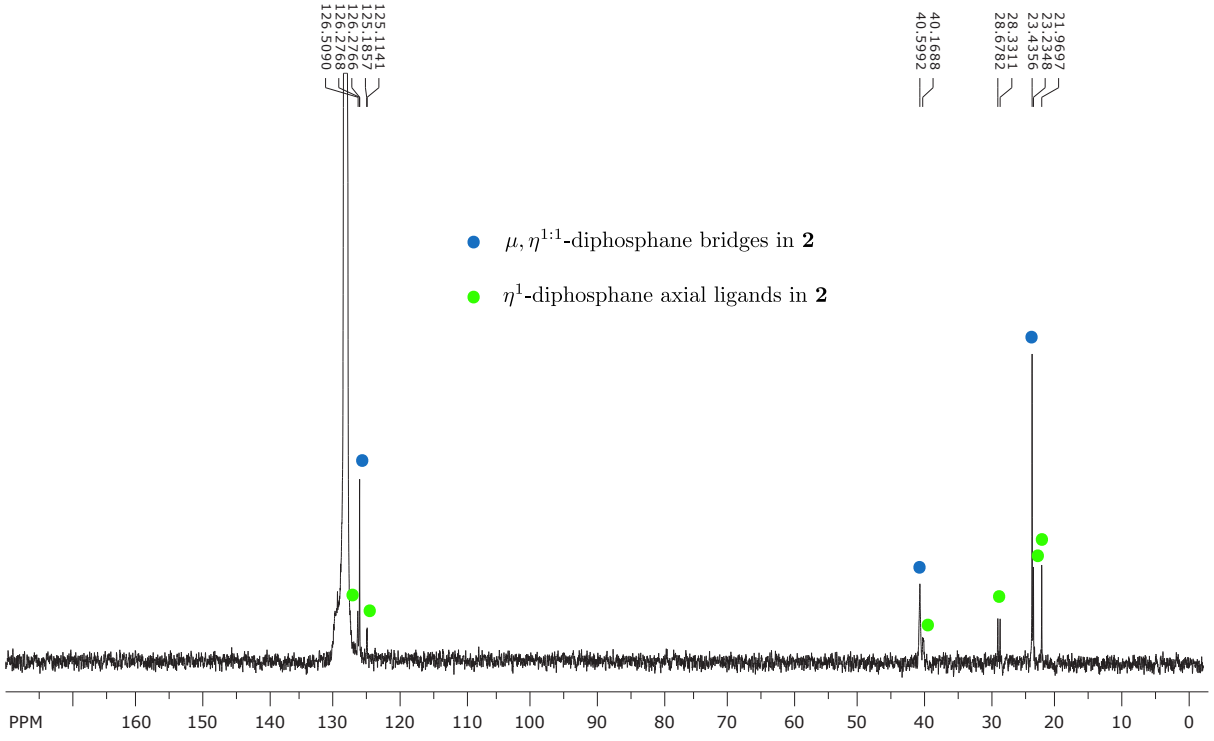

Figure S.3: $^{13}C\{^{1}H\}$ NMR spectrum of complex **2**.

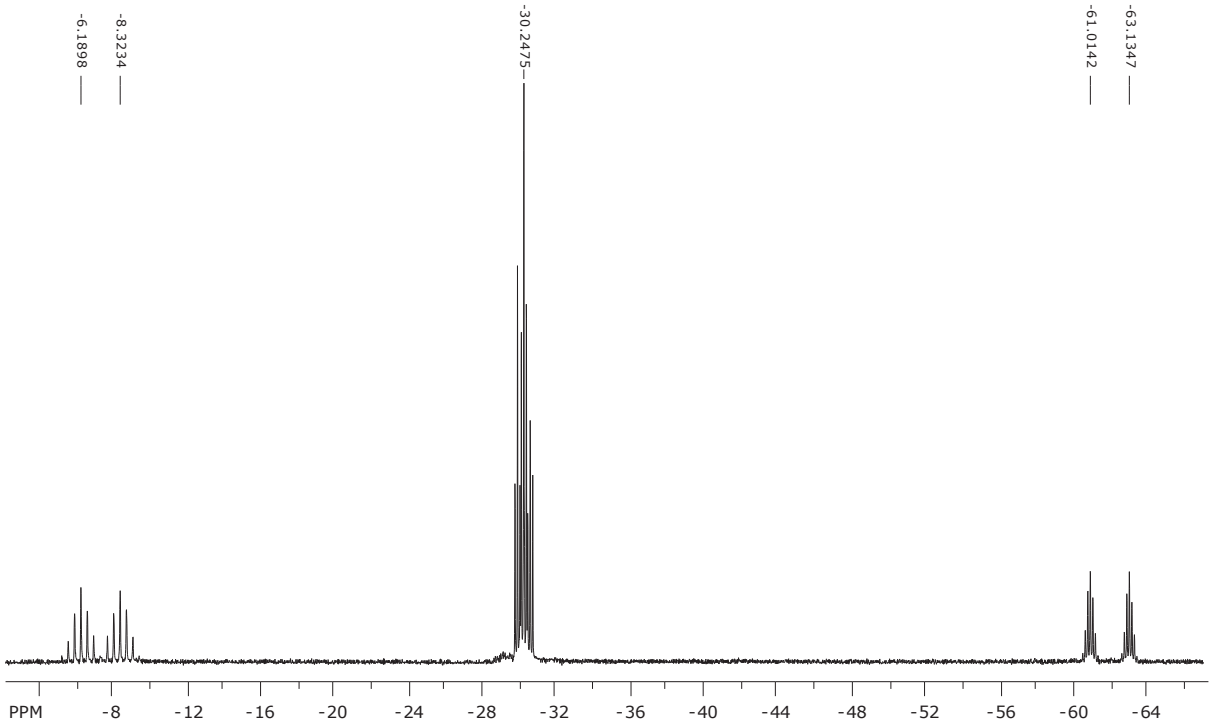

Figure S.4: $^{31}P\{^{1}H\}$ NMR spectrum of complex **2**.

S.1.3 Synthesis of Complex $(Ph_3P)Ni(\mu\text{-}1)_3Ni(PPh_3)$ (3-Ni)

A toluene (7 mL) solution containing PPh_3 (389 mg, 1.48 mmol, 2.0 equiv) and **1** (503 mg, 2.28 mmol, 3.0 equiv) was added drop-wise to a toluene (13 mL) solution of $Ni(cod)_2$ (408 mg, 1.48 mmol, 2.0 equiv). During the addition, the color changed from bright yellow to dark orange. The resulting mixture was stirred for one hour during which an orange precipitate formed. The mixture was stored overnight at –35 °C and the precipitate was isolated on a fritted glass filter, washed with cold pentane, and dried under reduced pressure (705 mg). Volatiles from the filtrate were removed under reduced pressure and toluene (8 mL) and Et_2O (2 mL) were added to the obtained residue. The precipitate (157 mg) was isolated from this mixture after storing it at –35 °C. The bright orange solids that were isolated (862 mg in total, 0.65 mmol, 89% yield) consisted of analytically pure complex **3**-Ni. ^{1}H NMR (C_6D_6, 20 °C, 500 MHz) δ: 7.91 (t, $^3J_{HH} = {}^3J_{HP} = 7.8$ Hz, 12 H, *o*-Ph), 7.22, (t, $^3J_{HH} = 7.3$ Hz, 12 H, *m*-Ph), 7.12 (t, $^3J_{HH} = 7.7$ Hz, 6 H, *p*-Ph), 2.38 (brd, $^2J_{HH} = 13.8$ Hz, 12 H, C*H*H), 2.31 (brd, 12 H, CH*H*), 1.63 (s, 36 H, CH_3) ppm (Figure S.5). ^{13}C{^{1}H} NMR (C_6D_6, 20 °C, 100.6 MHz) δ: 134.6 (d, $^1J_{CP} = 16.6$ Hz, *i*-Ph), 128.7 (*o*-Ph), 128.3, 128.1, 126.7 (*C*H$_0$), 38.3 (brs, *C*H$_2$), 23.0 (*C*H$_3$) ppm (Figure S.6). ^{31}P{^{1}H} NMR (C_6D_6, 20 °C, 161.9 MHz) δ: +36.7 (vsept, $J_{P_AP_X} = 48.4$ Hz, 2 P, P_APh$_3$), –31.6 (vt, 6 P, **1**) ppm (Figure S.7). Elemental analysis [%] found (and calcd. for $C_{72}H_{90}Ni_2P_8$): C 65.48 (65.48); H 6.94 (6.87); N none (0.00); P 18.78 (18.76). Decomposition temperature (from DSC): > 210 °C.

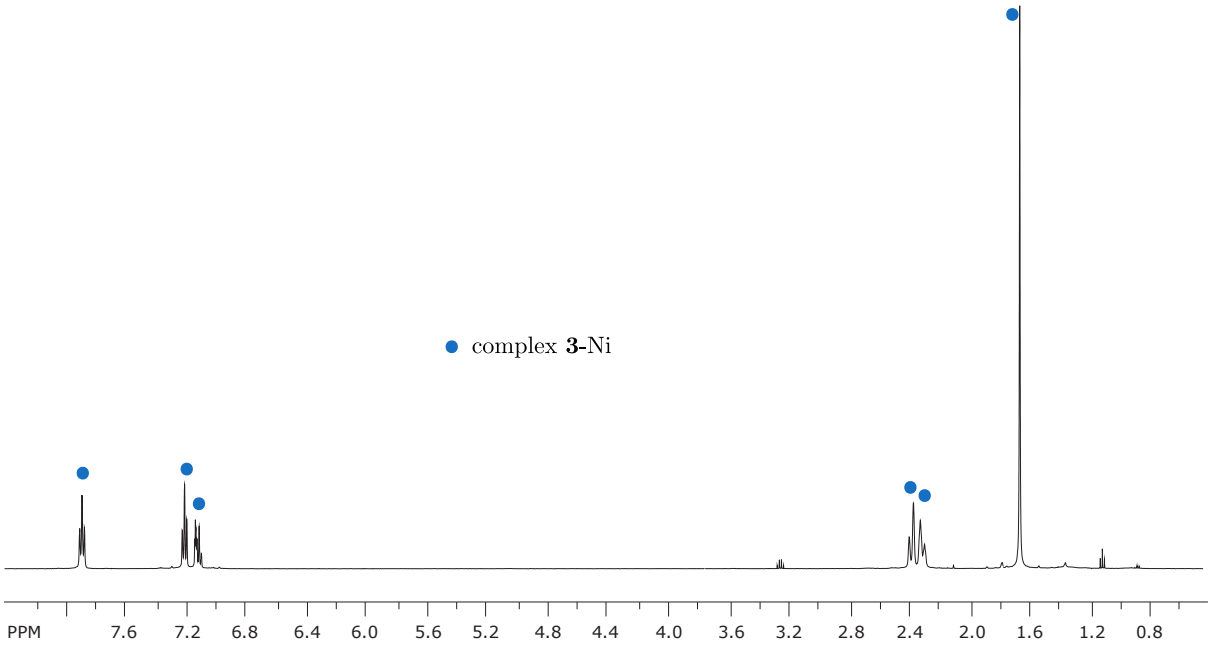

Figure S.5: ^{1}H NMR spectrum of complex **3**-Ni.

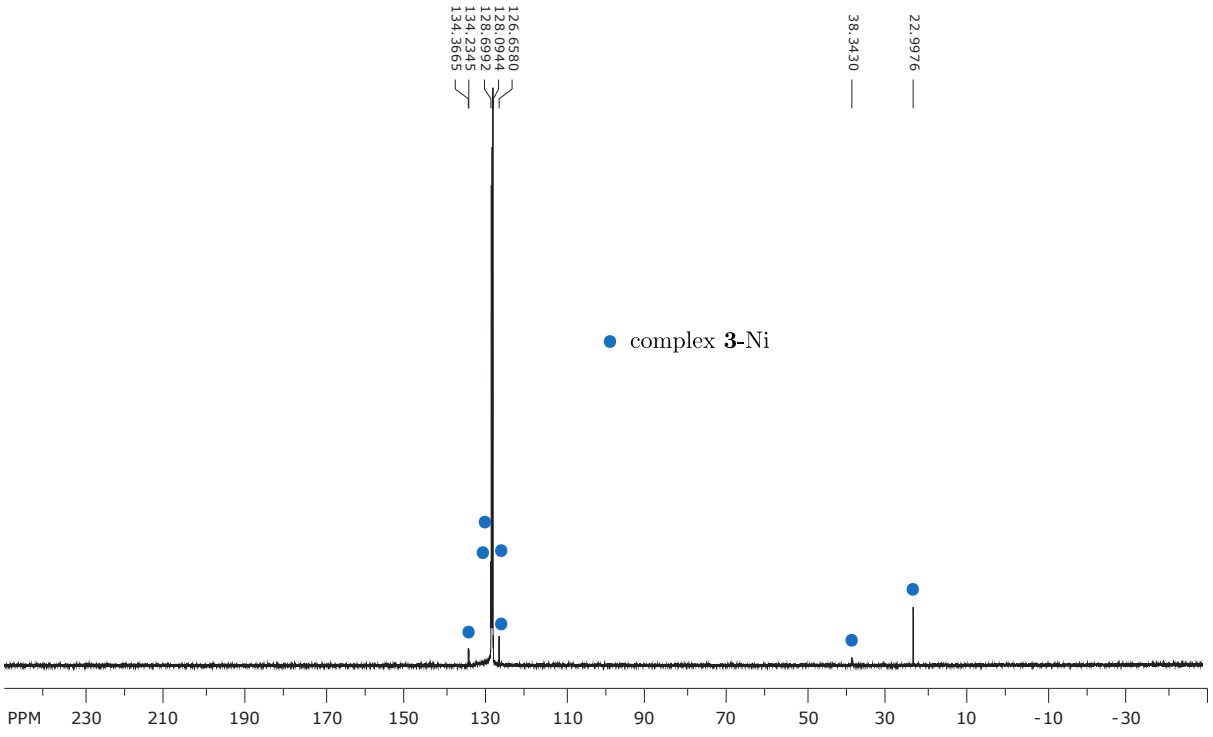

Figure S.6: $^{13}C\{^{1}H\}$ NMR spectrum of complex **3**-Ni.

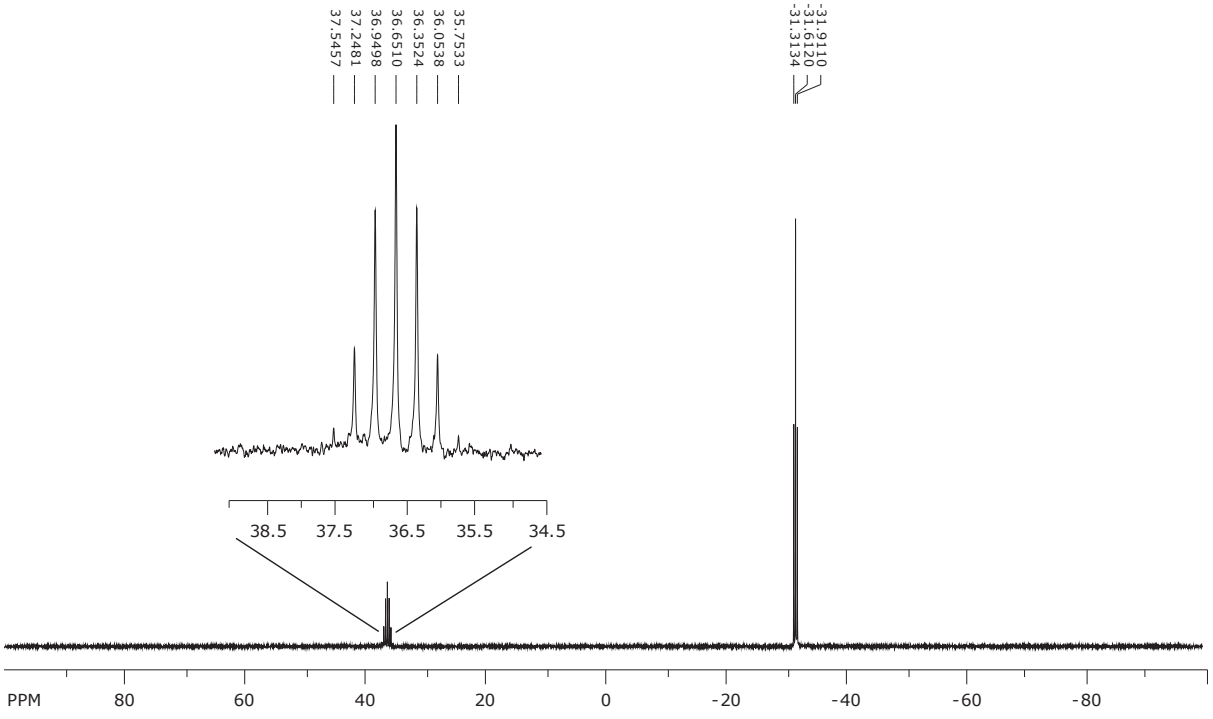

Figure S.7: $^{31}P\{^{1}H\}$ NMR spectrum of complex **3**-Ni.

S.1.4 Synthesis of Complex $(Ph_3As)Ni(\mu\text{-}1)_3Ni(AsPh_3)$ (4)

A toluene (20 mL) solution containing $AsPh_3$ (451 mg, 1.47 mmol, 2.0 equiv) and **1** (500 mg, 2.21 mmol, 3.0 equiv) was added drop-wise, over 5 mins, to a freshly prepared, stirring toluene (30 mL) solution of $Ni(cod)_2$ (405 mg, 1.47 mmol, 2.0 equiv). During the addition, the color changed from bright yellow to orange and eventually to dark brown. After stirring for one hour, the solution was diluted with pentane (50 mL) and stirred for another 15 minutes. A bright yellow precipitate formed, which was isolated on a fritted glass filter, washed with copious amounts of pentane (20 mL) and diethyl ether (10 mL), and dried under reduced pressure (582 mg). Volatiles from the filtrate were removed under reduced pressure and pentane was added to the resulting residue. The mixture was stirred, and the precipitate was isolated on the fritted glass filter, washed with diethyl ether, and dried for a second batch (331 mg). A total of 913 mg (0.65 mmol, 88% yield) of bright yellow-orange solids containing analytically pure complex **4** were isolated. ^{1}H NMR (C_6D_6, 20 °C, 500 MHz) δ: 7.91 (dd, $^3J_{HH}$ = 6.9 Hz, $^4J_{HH}$ = 1.3 Hz, 12 H, *o*-Ph), 7.21, (t, $^3J_{HH}$ = 7.4 Hz, 12 H, *m*-Ph), 7.13 (tt, $^3J_{HH}$ = 7.4 Hz, $^4J_{HH}$ = 1.5 Hz, 6 H, *p*-Ph), 2.41 (brd, $^2J_{HH}$ = 13.8 Hz, 12 H, C*H*H), 2.31 (brd, 12 H, CH*H*), 1.62 (s, 36 H, CH_3) ppm (Figure S.8).^{13}C{^{1}H} NMR (C_6D_6, 20 °C, 100.6 MHz) δ: 140.6 (*i*-Ph), 134.5 (*o*-Ph), 129.4 (*m*-Ph), 129.0 (*p*-Ph), 126.6 (CH_0), 39.3 (brs, CH_2), 23.0 (CH_3) ppm (Figure S.9). ^{31}P{^{1}H} NMR (C_6D_6, 20 °C, 161.9 MHz) δ: –28.2 ppm (Figure S.10). Elemental analysis [%] found (and calcd. for $C_{72}H_{90}Ni_2As_2P_6$): C 60.92 (61.39); H 6.32 (6.44); N none (0.00); P 13.49 (13.19). Decomposition temperature (from DSC): > 185 °C.

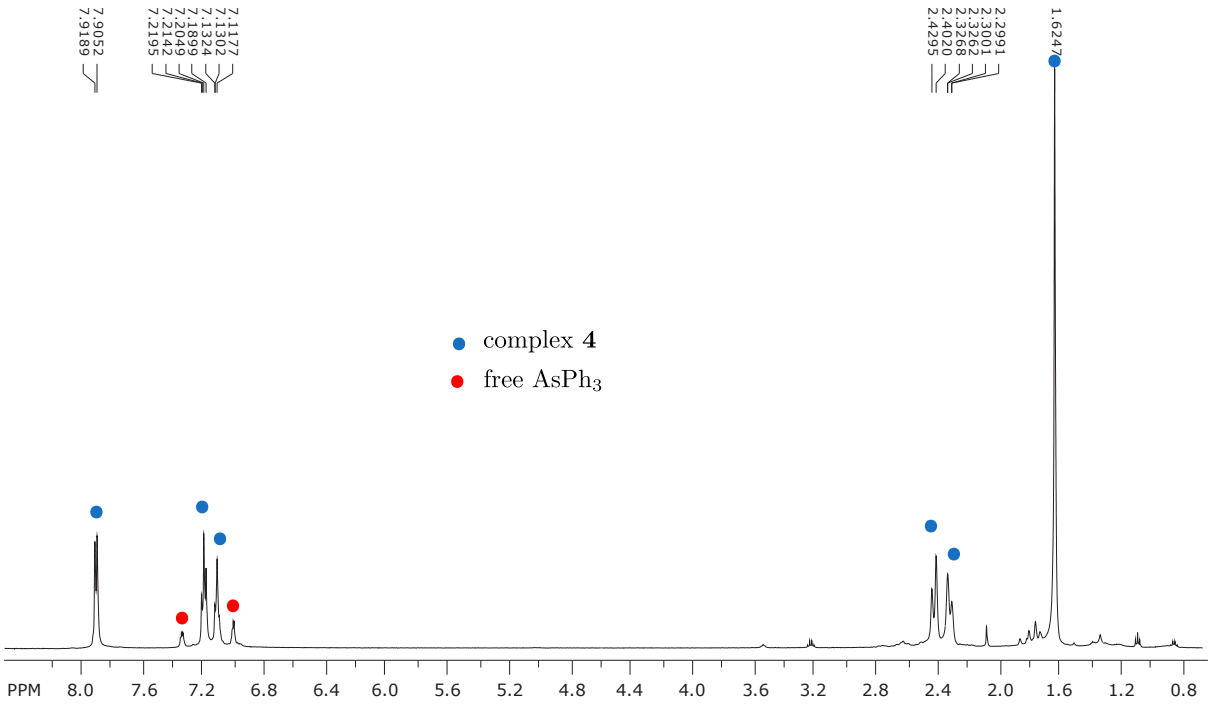

Figure S.8: ^{1}H NMR spectrum of isolated pure complex **4** indicating presence of dissociated $AsPh_3$.

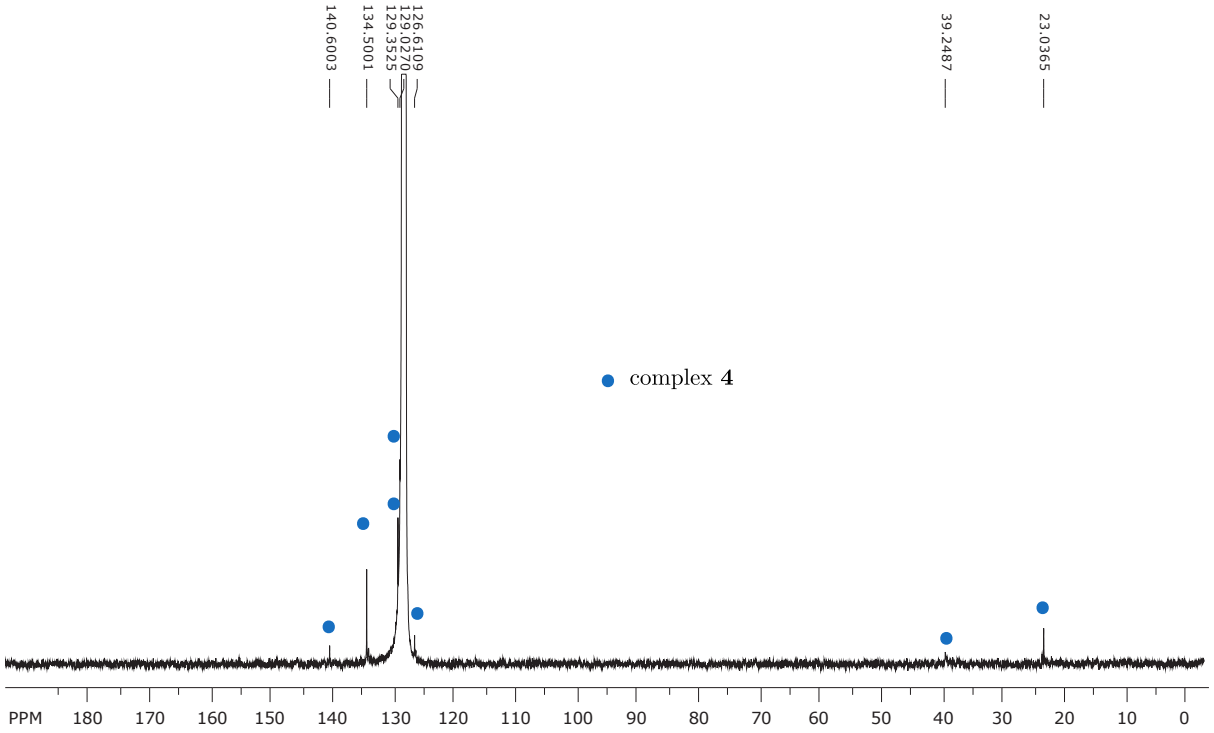

Figure S.9: $^{13}C\{^{1}H\}$ NMR spectrum of complex **4**.

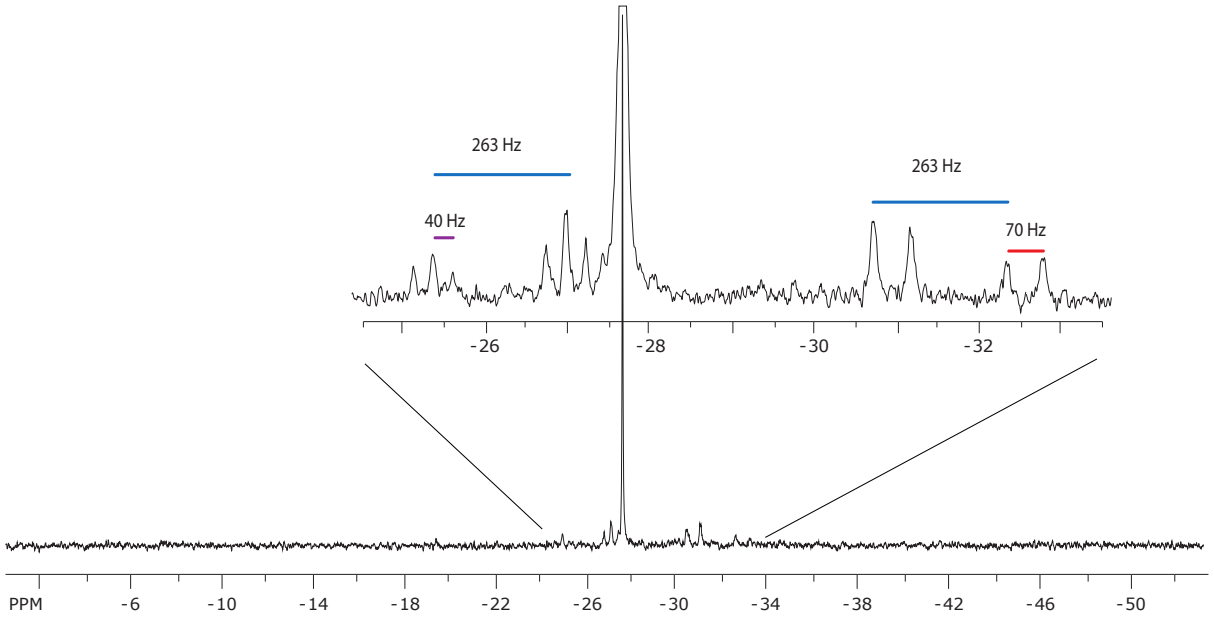

Figure S.10: $^{31}P\{^{1}H\}$ NMR spectrum of complex **4** in pyridine-d_5 showing presence of multiplets consistent with dissociated $(Ph_3As)Ni(\mu\text{-}\mathbf{1})_3Ni$(solvent) species.

S.1.5 Synthesis of Complex $(Ph_3Sb)Ni(\mu\text{-}1)_3Ni(SbPh_3)$ (5)

A toluene (5 mL) solution containing $SbPh_3$ (131 mg, 0.371 mmol, 2.0 equiv) and **1** (125 mg, 0.552 mmol, 3.0 equiv) was added drop-wise to a freshly prepared, stirring toluene (2 mL) solution of $Ni(cod)_2$ (102 mg, 0.373 mmol, 2.0 equiv). The mixture changed color from bright yellow to orange and then to dark brown. Within 2 mins, an orange precipitate started forming, and the mixture was stirred for another hour at which point pentane (5 mL) was added to crash out further solids. These were collected on a fritted glass filter, washed with pentane and diethyl ether, dried and weighed, yielding bright orange solids containing analytically pure complex **5** (234 mg, 0.162 mmol, 87% yield). ^{1}H NMR (C_6D_6, 20 °C, 500 MHz) δ: 8.02 (d, $^3J_{HH}$ = 7.7 Hz, 12 H, *o*-Ph), 7.26, (t, $^3J_{HH}$ = 7.0 Hz, 12 H, *m*-Ph), 7.18 (t, $^3J_{HH}$ = 7.6 Hz, 6 H, *p*-Ph), 2.51 (brd, $^2J_{HH}$ = 14.4 Hz, 12 H, C*H*H), 2.39 (brd, 12 H, CH*H*), 1.63 (s, 36 H, CH_3) ppm (Figure S.11). ^{31}P{^{1}H} NMR (C_6D_6, 20 °C, 161.9 MHz) δ: –21.6 ppm (Figure S.12). ^{13}C NMR spectra of complex **5** could not be obtained due to its very low solubility. At room temperature, it completely crystallizes out of benzene solutions in less than 30 mins, while at temperatures around 80°Cit decomposes rapidly. In dimethylsulfoxide, acetonitrile, THF, or fluorobenzene it is highly insoluble, while in chloroform it decomposes. Elemental analysis [%] found (and calcd. for $C_{72}H_{90}Ni_2Sb_2P_6$): C 57.49 (57.57); H 5.92 (6.04); N none (0.00); P 12.41 (12.37). Decomposition temperature (from DSC): > 190 °C.

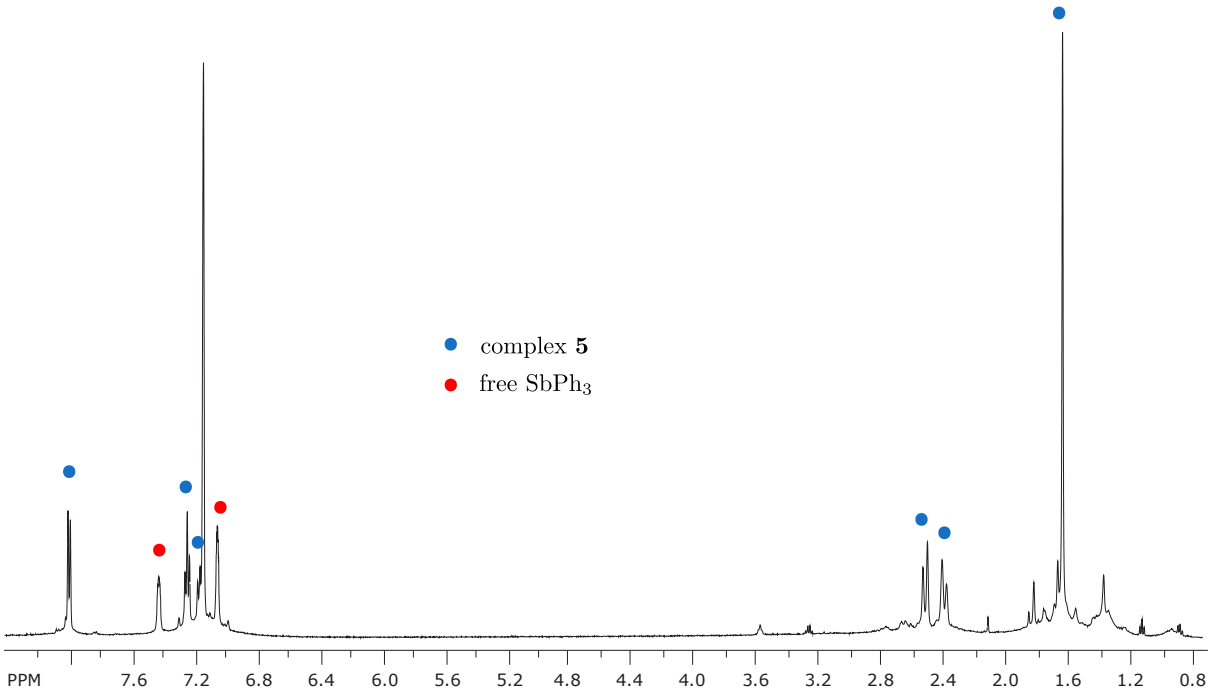

Figure S.11: ^{1}H NMR spectrum of isolated pure complex **5** indicating presence of dissociated $SbPh_3$.

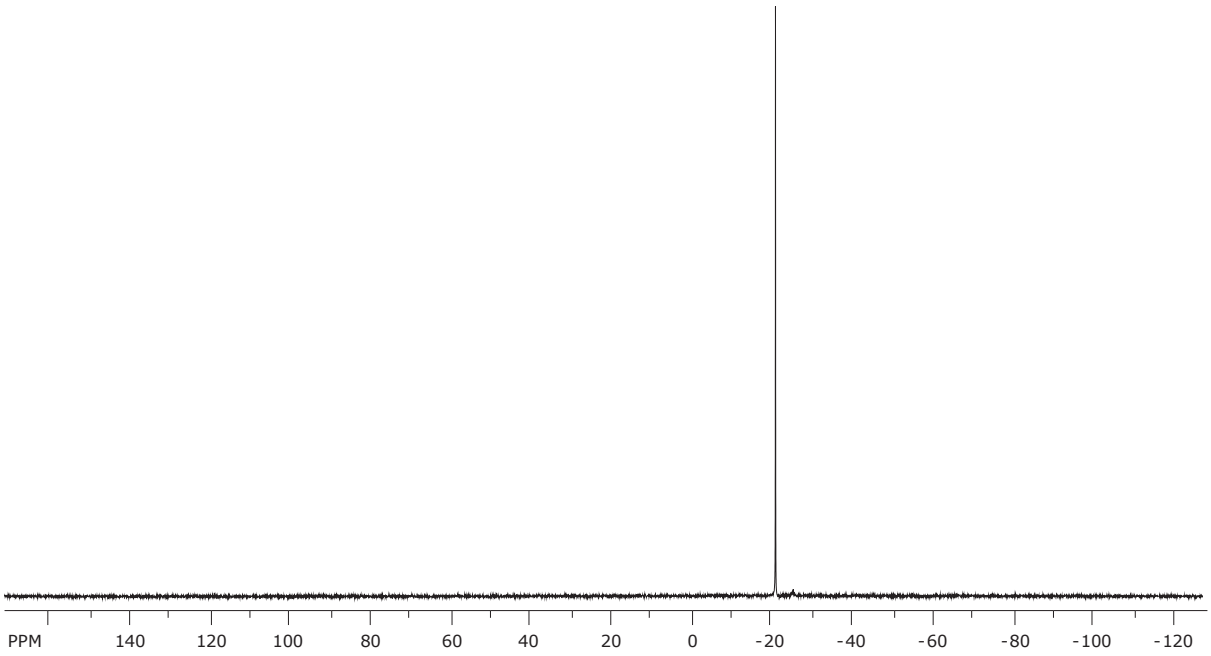

Figure S.12: $^{31}P\{^{1}H\}$ NMR spectrum of complex **5**.

S.1.6 Synthesis of Complex $(Ph_3P)Pd(\mu\text{-}1)_3Pd(PPh_3)$ (3-Pd)

A toluene (2 mL) solution of **1** (86 mg, 0.38 mmol, 3.0 equiv) was added to a clear, yellow solution of $Pd(PPh_3)_4$ (292 mg, 0.25 mmol, 2.0 equiv) in toluene (15 mL) and the resulting mixture was stirred for one hour, leading to the formation of small amounts of a yellow precipitate. Pentane (1 mL) was added and the resulting mixture was stored at –35 °C. The precipitate was isolated on a fritted glass filter, washed with pentane, and dried under reduced pressure to yield bright yellow solids containing analytically pure complex **3**-Pd (117 mg, 0.083 mmol, 65% yield). ^{1}H NMR (C_6D_6, 20 °C, 500 MHz) δ: 7.97 (brs, 12 H, *o*-Ph), 7.24, (brs, 12 H, *m*-Ph), 7.12 (brs, 6 H, *p*-Ph), 2.41 (brd, $^{2}J_{HH}$ = 13.3 Hz, 12 H, C*H*H), 2.22 (brd, 12 H, CH*H*), 1.69 (s, 36 H, CH_3) ppm (Figure S.13). ^{13}C NMR (C_6D_6, 80°C, 125.8 MHz) δ: 134.6 (d, $^{1}J_{CP}$ = 19.0 Hz, *i*-Ph), 128.9, 128.7, 128.2, 126.3 (CH_0), 37.3 (brs, CH_2), 22.6 (CH_3) ppm. $^{31}P\{^{1}H\}$ NMR (C_6D_6, 20 °C, 161.9 MHz) δ: +31.2 (vsept, $J_{P_AP_X}$ = 56.8 Hz, 2 P, P_APh_3), –33.7 (vt, 6 P, **1**) ppm (Figure S.14). Elemental analysis [%] found (and calcd. for $C_{72}H_{90}Pd_2P_8$): C 61.17 (61.07); H 6.41 (6.41); N none (0.00); P 17.35 (17.50). Decomposition temperature (from DSC): > 205 °C.

S.1.7 Synthesis of Complex $(Ph_3P)Pt(\mu\text{-}1)_3Pt(PPh_3)$ (3-Pt)

A toluene (2 mL) solution of **1** (98.8 mg, 0.437 mmol , 3.0 equiv) was added to a clear, pale-orange solution of $Pt(PPh_3)_4$ (362.4 mg, 0.291 mmol, 2.0 equiv) in toluene (8 mL). During the addition, the color darkened to intense orange. The mixture was stirred for one hour, after which it was layered with 10 mL pentane and stored at –35 °C. The precipitate that formed was isolated on a fritted glass filter, washed with pentane, and dried under reduced

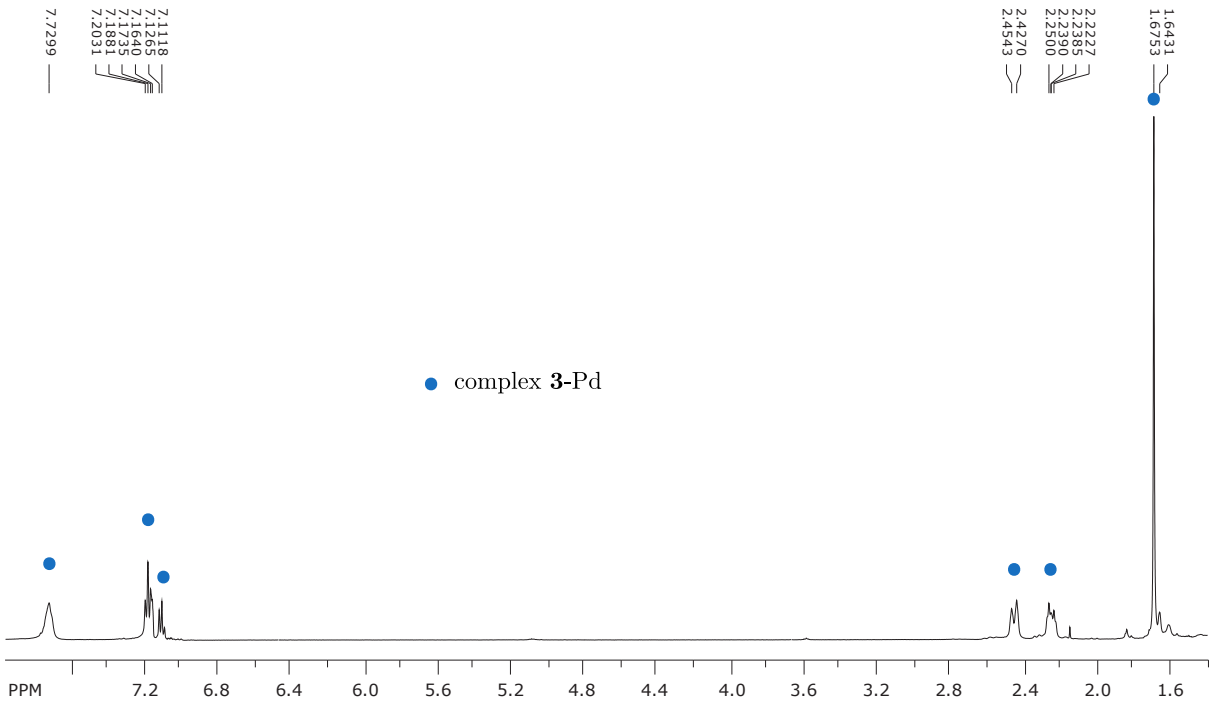

Figure S.13: ^{1}H NMR spectrum (80°C, C_6D_6) of complex **3**-Pd.

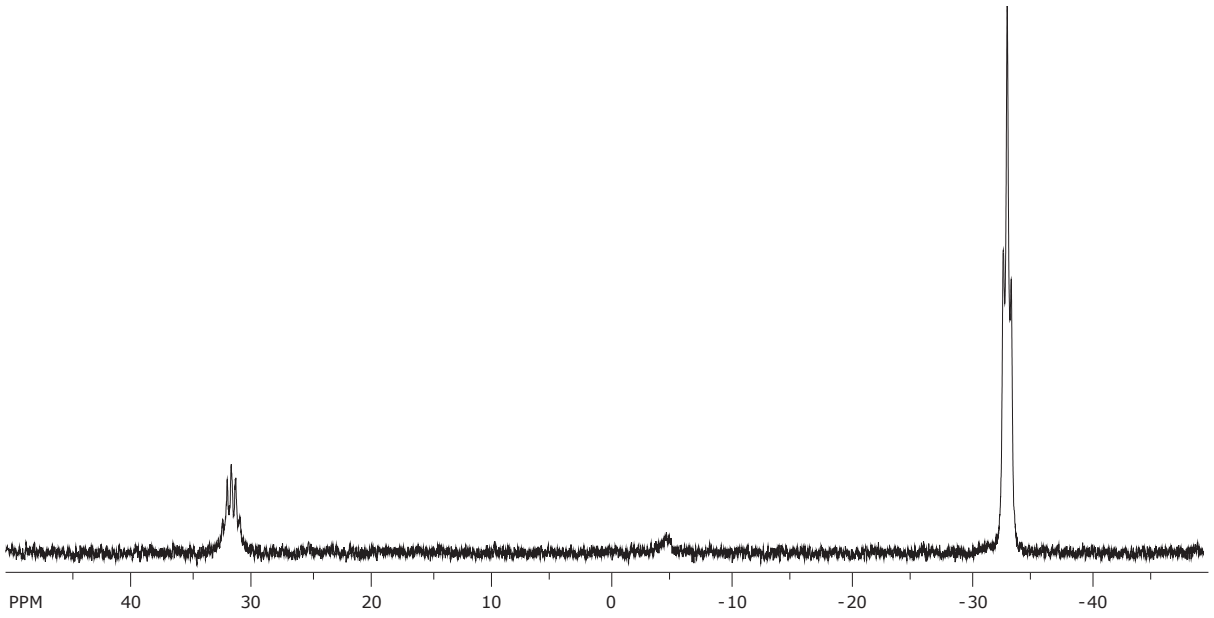

Figure S.14: $^{31}P\{^{1}H\}$ NMR spectrum (60°C, C_6D_6) of complex **3**-Pd .

pressure to yield bright yellow solids of analytically pure complex **3**-Pt (211 mg, 0.132 mmol, 91% yield). ^{1}H NMR (C_6D_6, 20 °C, 500 MHz) δ: 7.97 (t, $^{3}J_{HH}$ = $^{3}J_{HP}$ = 8.4 Hz, 12 H, *o*-Ph), 7.25, (t, $^{3}J_{HH}$ = 7.4 Hz, 12 H, *m*-Ph), 7.12 (t, $^{3}J_{HH}$ = 7.3 Hz, 6 H, *p*-Ph), 2.50 (brd, $^{2}J_{HH}$ = 13.5 Hz, 12 H, C*H*H), 2.39 (brd, 12 H, CH*H*), 1.65 (s, 36 H, CH_3) ppm (Figure S.15). ^{13}C NMR (C_6D_6, 60°C, 125.8 MHz) δ: 134.7 (d, $^{1}J_{CP}$ = 16.7 Hz, *i*-Ph), 129.3, 128.3, 128.2, 126.8 (*C*H$_0$), 41.7 (brs, *C*H$_2$), 23.1 (*C*H$_3$) ppm (Figure S.16). ^{31}P{^{1}H} NMR (C_6D_6, 20 °C, 161.9 MHz) δ: +26.8 (d-vsept, $J_{P_AP_X}$ = 79.3 Hz, $^{1}J_{^{31}P_A\,^{195}Pt}$ = 4650 Hz, 2 P, *P*$_A$Ph$_3$), –45.3 (vt, $^{1}J_{^{31}P_X\,^{195}Pt}$ = 3510 Hz, $^{2}J_{^{31}P_X\,^{195}Pt}$ = 379 Hz, 6 P, **1**) ppm (Figure S.17). Elemental analysis [%] found (and calcd. for $C_{72}H_{90}Pt_2P_8$): C 54.32 (54.27); H 5.55 (5.69); N none (0.00); P 15.42 (15.55).

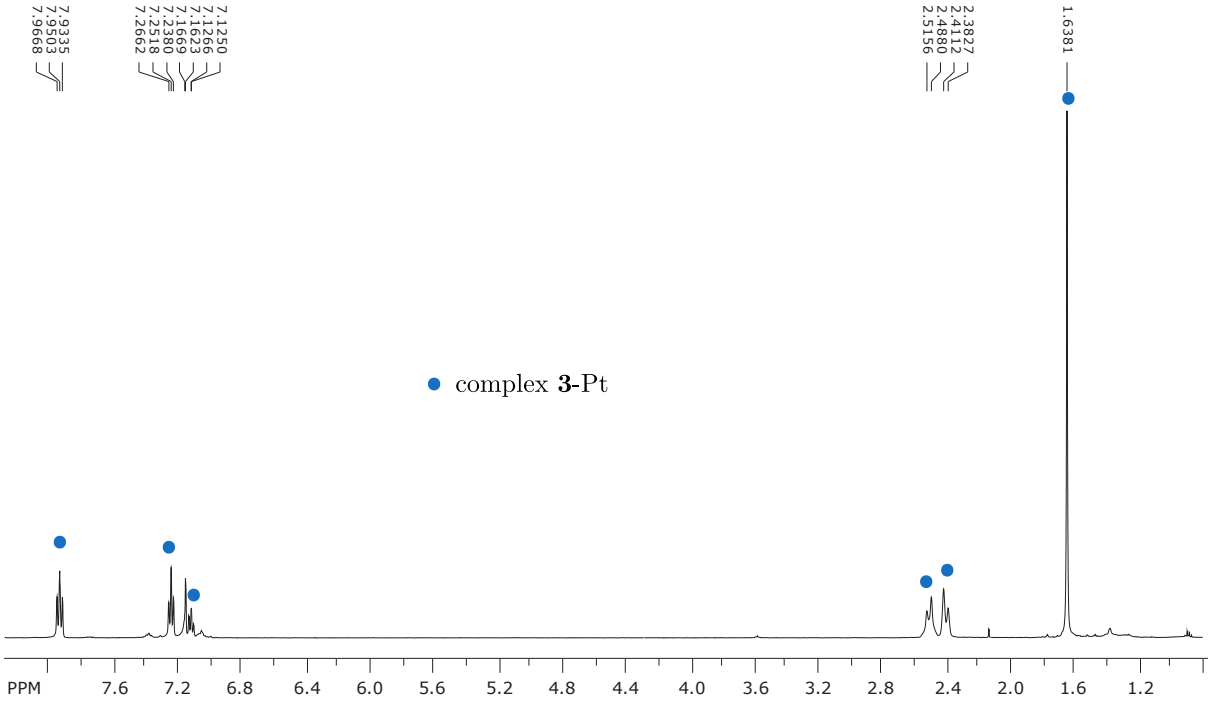

Figure S.15: ^{1}H NMR spectrum of complex **3**-Pt.

S.1.8 Streamlined Synthesis of Diphosphane 1

A recycled sample of P_4 (1.17 g, ca. 9.4 mmol, ca. 2.1 equiv) was stirred in hexane (120 mL) for a 1–2 h after which the yellow suspension was filtered through a short layer of alumina (0.5 cm). The alumina was washed with hexane (10 mL) and the resulting clear filtrate was placed in a 250 mL quartz round bottom flask (ChemGlass) together with 2,3-dimethylbutadiene (2.0 mL, 1.45 g, 17.7 mmol, 4 equiv). The flask was equipped with a vacuum valve, partially degassed and sealed securely before being brought outside of the glovebox. The mixture was irradiated in using a Rayonet photochemical reactor (RPR-200, Southern New England Ultra Violet Company) loaded with 16 RPR-2537 Å lamps, each emitting ca. 35 W at 253.7 nm (spectral output was reported previously[2]). A cooling

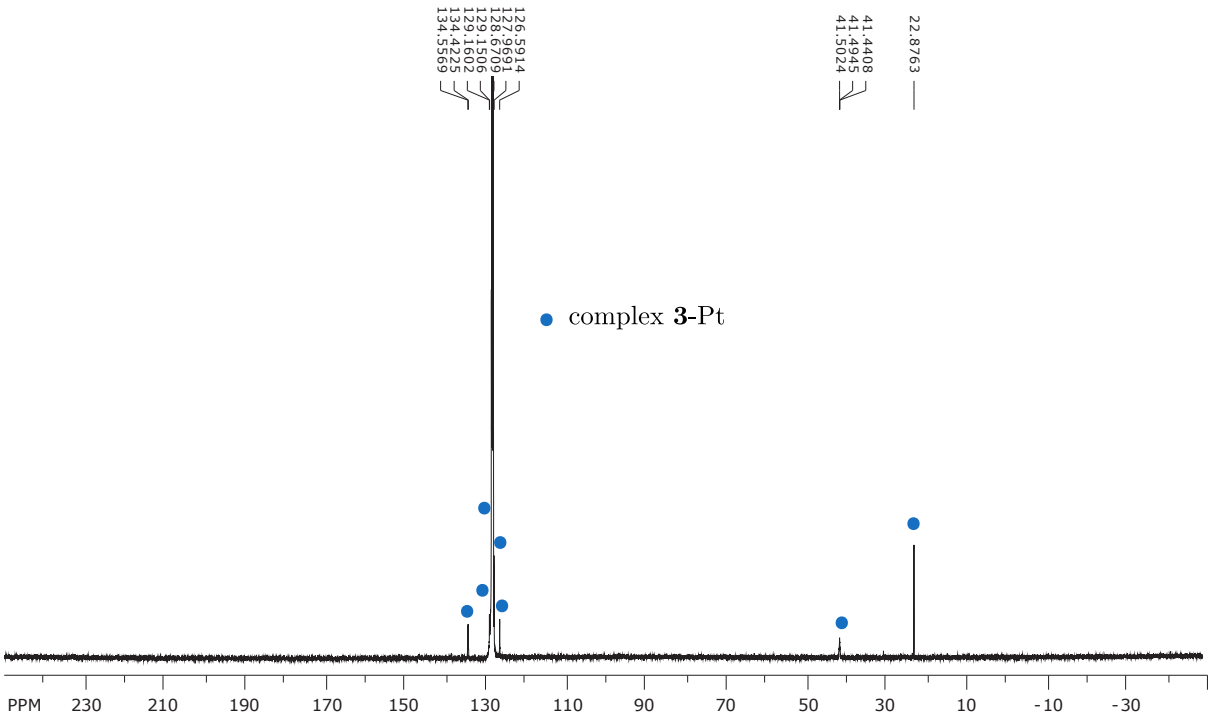

Figure S.16: $^{13}C\{^{1}H\}$ NMR spectrum (60°C, C_6D_6) of complex **3**-Pt.

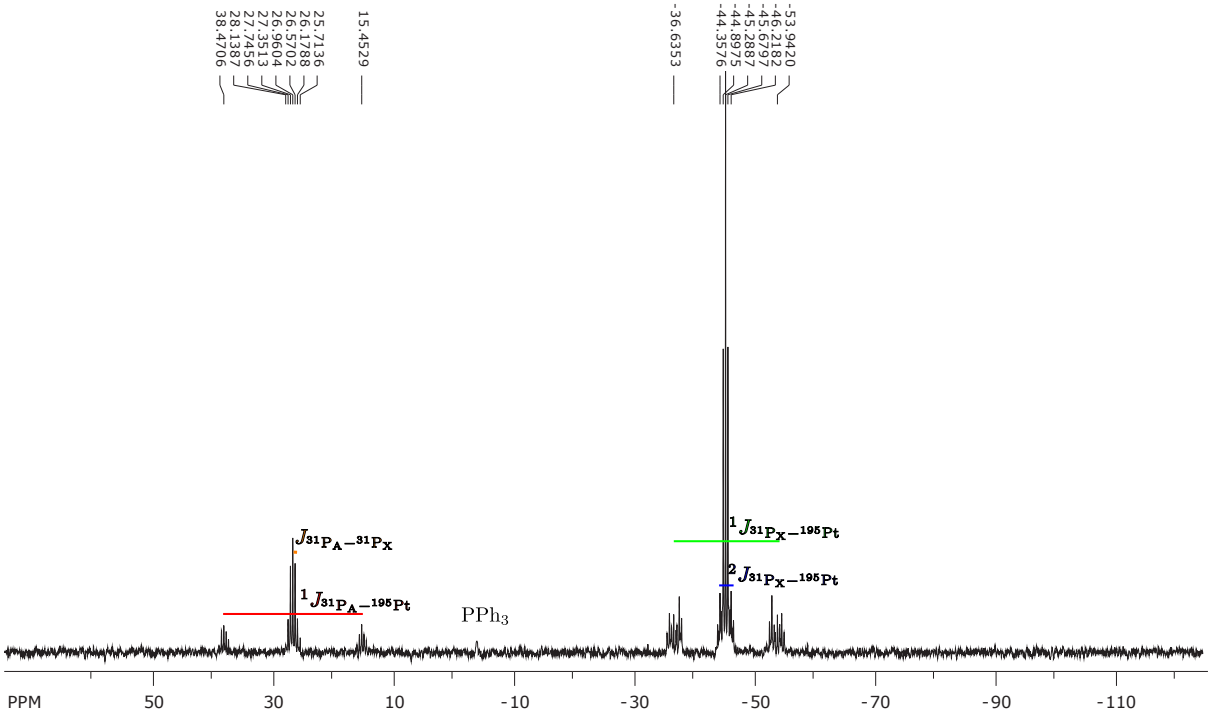

Figure S.17: $^{31}P\{^{1}H\}$ NMR spectrum (60°C, C_6D_6) complex **3**-Pt showing measured coupling constants.

fan was used to keep the temperature inside the photolysis chamber at ca. 55–65°C in order to prevent the P_4 from condensing above the solution and form a yellow coating which would block the UV radiation from reaching the solution. After irradiating for 14–16 hours, the resulting yellow suspension was cooled and brought back into the glovebox. The procedure was repeated two times and the resulting mixtures were worked-up at the same time.

Each batch was passed separately through a layer of alumina (2 cm) and washed with pentane (50 mL) to remove the unreacted P_4. The after removing under vacuum the volatiles from the pentane filtrates, a white solid consisting of mostly P_4 (ca. 1.5 g, ca. 40% of the total amount used) was recovered, which can be reused for other photolytic batches. The alumina layers were washed with diethyl ether (150 mL each) and the three resulting pale-yellow filtrates were merged together. After removing the volatiles from the diethyl ether washings under vacuum, a pale-yellow solid was obtained (ca. 3.5 g). This was dissolved in hot toluene (ca. 8 mL) and the resulting solution was allowed to cool down and stored at –35°C for about 12 hours. The colorless crystals were collected on a fritted glass filter, washed with cold pentane, dried, and weighted (ca. 1.0 g). The filtrate was redissolved in hot toluene (ca. 3 mL) and another batch (0.3 g) was obtained after storing at –35°C. A total of ca. 1.4–1.5 g (∼12% yield based on diene) of crystalline white solids of diphosphane **1** were collected after the third recrystallization.

S.1.9 Treatment of Complexes 4 and 5 with PPh_3

To a solution of **4** (24.0 mg, 0.017 mmol, 1.0 equiv) in THF (2 mL), PPh_3 (7.9 mg, 0.035 mmol, 2.0 equiv) was added as a solution in THF (0.5 mL). The mixture was stirred for 10 mins, without any obvious color change, and after 30 mins it was analyzed by ^{31}P NMR spectroscopy. This indicated complete, selective formation of complex **3**-Ni and the absence of unreacted PPh_3 (Figure S.18).

To a slurry of **5** (23.6 mg, 0.016 mmol, 1.0 equiv) in THF (2 mL), PPh_3 (7.9 mg, 0.030 mmol, 1.9 equiv) was added as a solution in THF (0.5 mL). The mixture was stirred for 10 mins, without any obvious change in the appearance of precipitate. A ^{31}P NMR spectrum was obtained of an aliquot after 30 mins of stirring the mixture in which incomplete formation of **3**-Ni complex could be observed. Signals for unreacted PPh_3 and **5** were also observed, together with multiplets around –20 ppm that are consistent with mixed $(Ph_3P)Ni(\mathbf{1})_3Ni(SbPh_3)$ species (Figure S.19).

S.1.10 Treatment of Complexes 3-Ni and 5 with 4

A suspension of complex **3**-Ni (11.2 mg, 0.0080 mmol, 1.0 equiv) in C_6D_6 (0.5 mL) was added to a stirring suspension of **4** (10.5 mg, 0.0101 mmol, 1.0 equiv) in C_6D_6 (0.5 mL) which let to the dissolution of most of the solids within a minute. NMR spectroscopic analysis indicated the presence of multiplets in the ^{31}P NMR spectrum consistent with $(Ph_3P)Ni(\mathbf{1})_3Ni(AsPh_3)$ species (Figure S.20).

A suspension of complex **5** (15.3 mg, 0.0101 mmol, 1.0 equiv) in C_6D_6 (0.5 mL) was added to a stirring

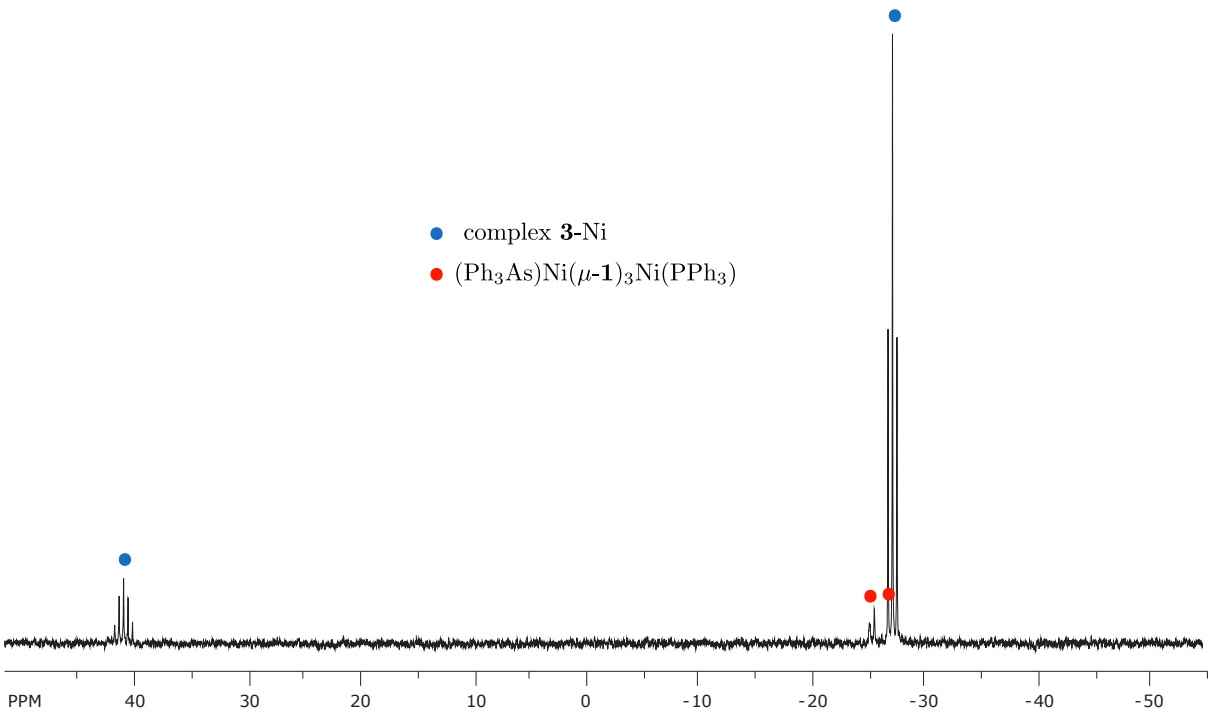

Figure S.18: $^{31}P\{^{1}H\}$ NMR spectrum (THF) of the reaction mixture of complex **4** with 2.0 equiv of PPh_3 after 20 mins of stirring.

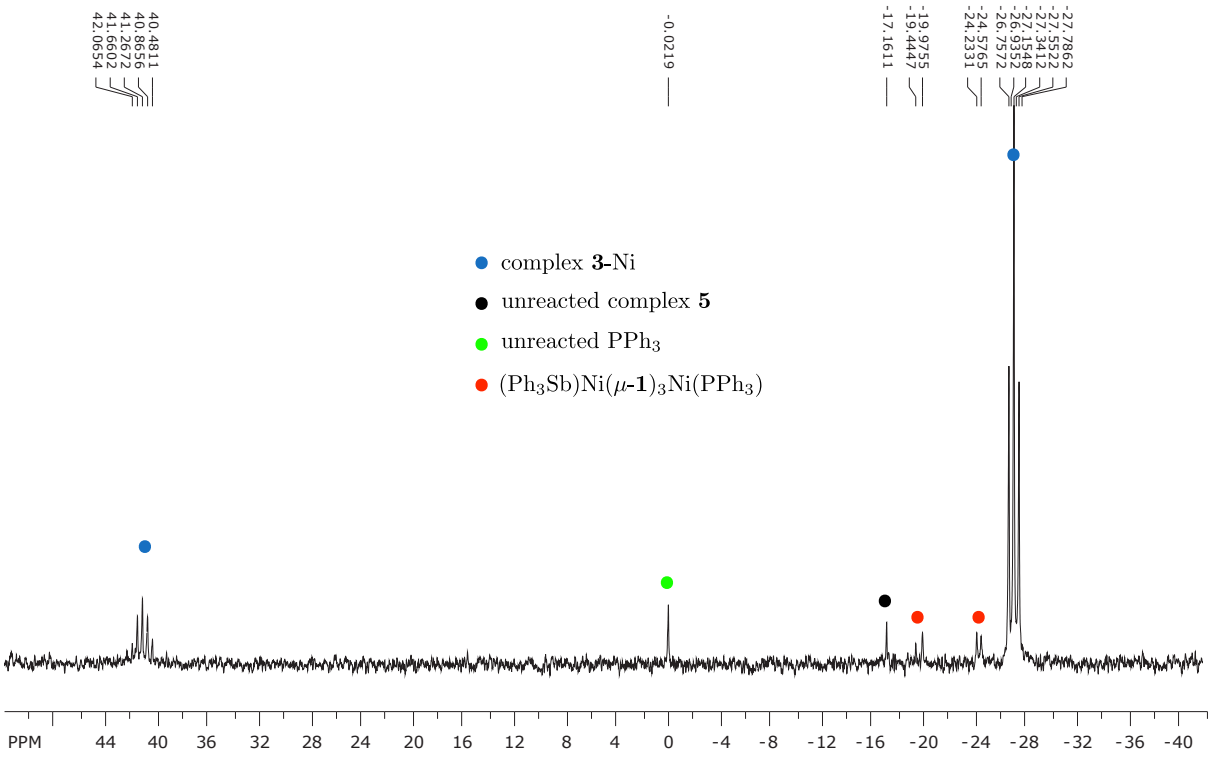

Figure S.19: $^{31}P\{^{1}H\}$ NMR spectrum (THF) of the reaction mixture of complex **5** with 1.9 equiv of PPh_3 after 20 mins of stirring.

suspension of **4** (14.3 mg, 0.0101 mmol, 1.0 equiv) in C_6D_6 (0.5 mL) which produced no obvious color change. The sample was stirred well and after 10 mins it was analyzed by NMR spectroscopy. The appearance of doublets in the ^{31}P NMR spectrum consistent with the $(Ph_3As)Ni(\mathbf{1})_3Ni(SbPh_3)$ complex was observed (Figure S.21).

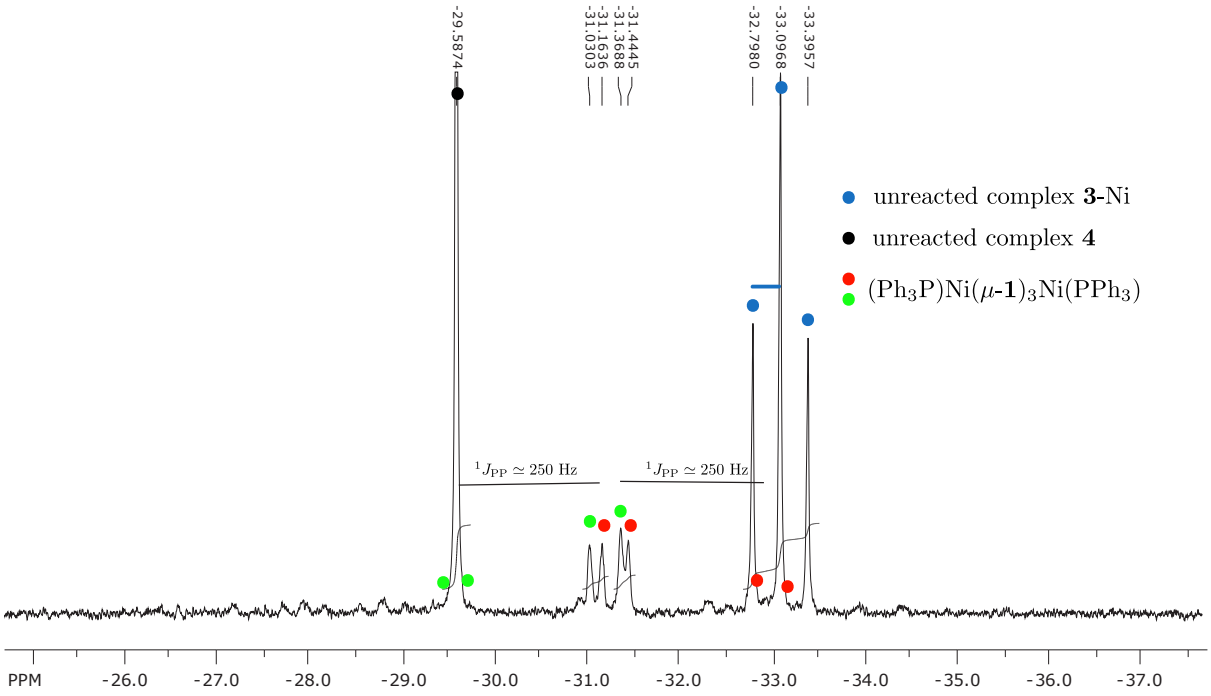

Figure S.20: A $^{31}P\{^1H\}$ NMR spectrum zoom (in THF) in the diphosphane region for the reaction mixture of complex **4** with complex **3**-Ni. Second-order coupling in the mixed-ligand complex (between doublets labeled in red and green) leads to the other half of the expected doublet to be obscured by the other peaks.

S.1.11 Treatment of $Ni(cod)_2$, $Pd(PPh_3)_4$ and $Pt(PPh_3)_4$ with P_2Ph_4

A suspension of P_2Ph_4 (55 mg, 0.15 mmol, 2.5 equiv) in C_6D_6 (0.5 mL) was added to a suspension of $Ni(cod)_2$ (17 mg, 0.06 mmol, 1.0 equiv) in C_6D_6 (0.5 mL) under stirring. The mixture turned immediately from yellow to orange, red, and then to brown. After 30 mins of stirring the mixture had turned green-brown. At this point, NMR spectroscopy indicated the presence of unreacted P_2Ph_4 and free 1,5-COD, but no other major NMR-active products (Figure S.22). After a day, green crystals had formed and were determined by X-ray diffraction spectroscopy to consist of the previously-reported complex $Ni(HPPh_2)_4$.[3]

A suspension of P_2Ph_4 (55 mg, 0.023 mmol, 1.5 equiv) in C_6D_6 (0.5 mL) was added to a pale yellow suspension of $Pd(PPh_3)_4$ (17 mg, 0.016 mmol, 1.0 equiv) in C_6D_6 (0.5 mL) under stirring. Upon addition, all the solids dissolved as the color of the mixture turned to orange and then to red. NMR spectra obtained after one hour revealed large amounts of free PPh_3 and P_2Ph_4, some unreacted $Pd(PPh_3)_4$,[4,5] but no ^{31}P NMR signals consistent with the formation of bimetallic species (Figure S.23).

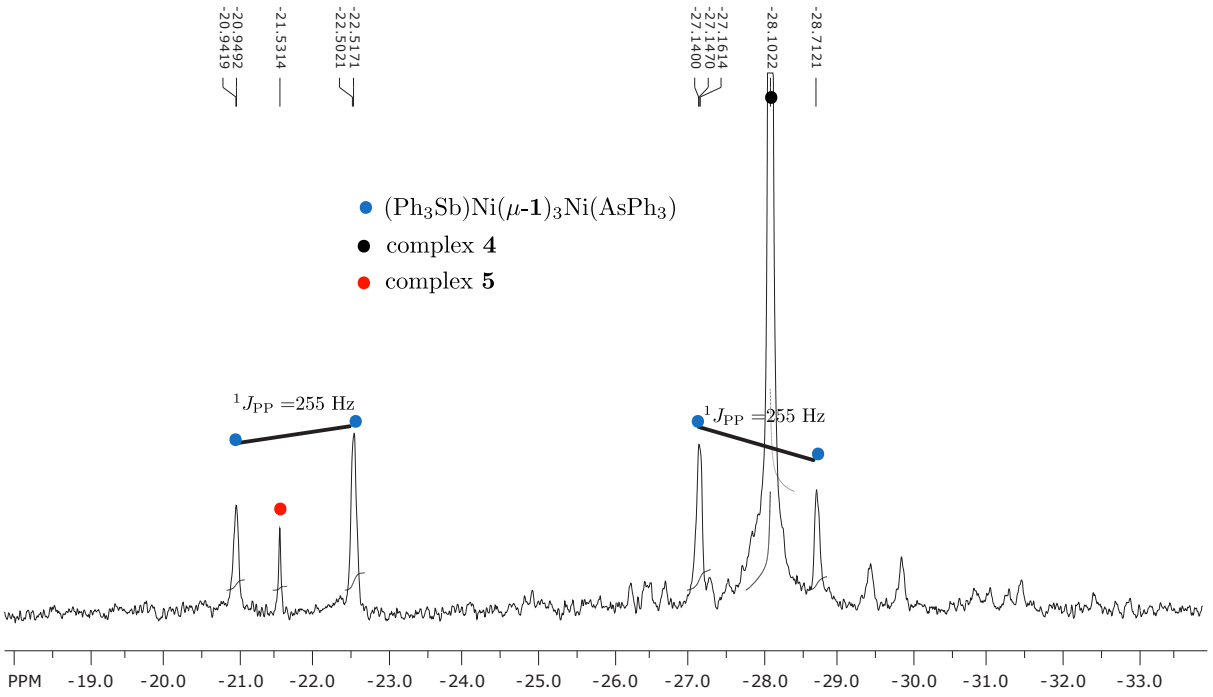

Figure S.21: A $^{31}P\{^{1}H\}$ NMR spectrum zoom (THF) in the diphosphane region for the reaction mixture of complex **4** with complex **5**.

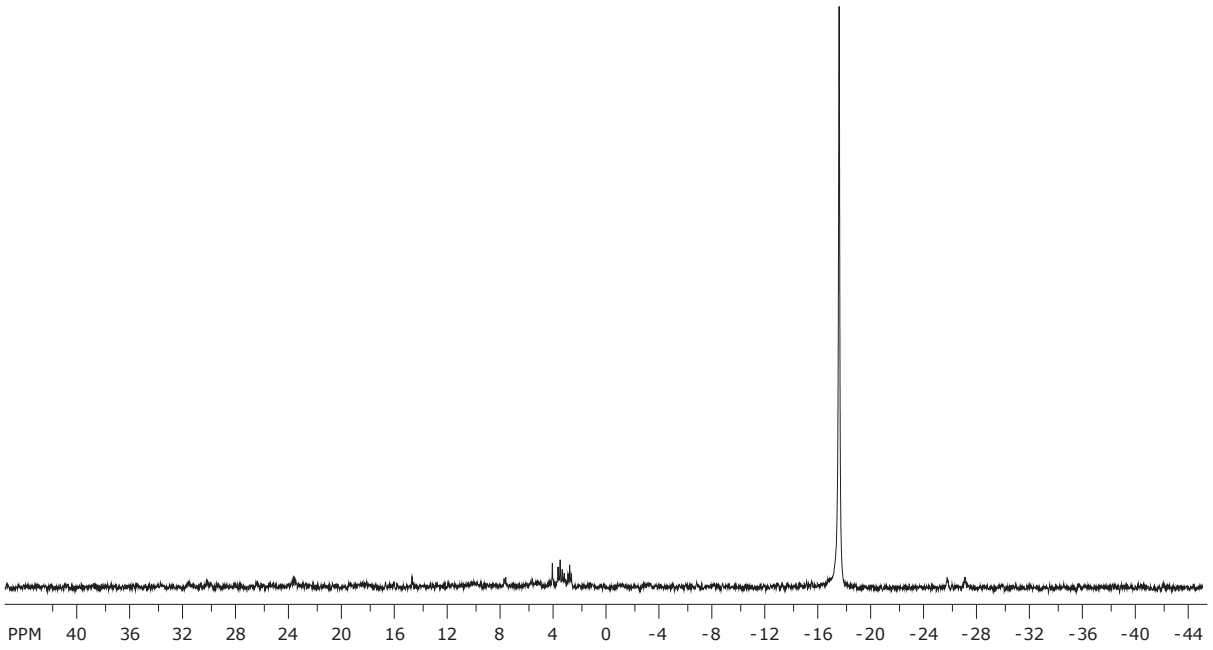

Figure S.22: $^{31}P\{^{1}H\}$ NMR spectrum of the reaction mixture between $Ni(cod)_2$ and P_2Ph_4 after one hour of stirring.

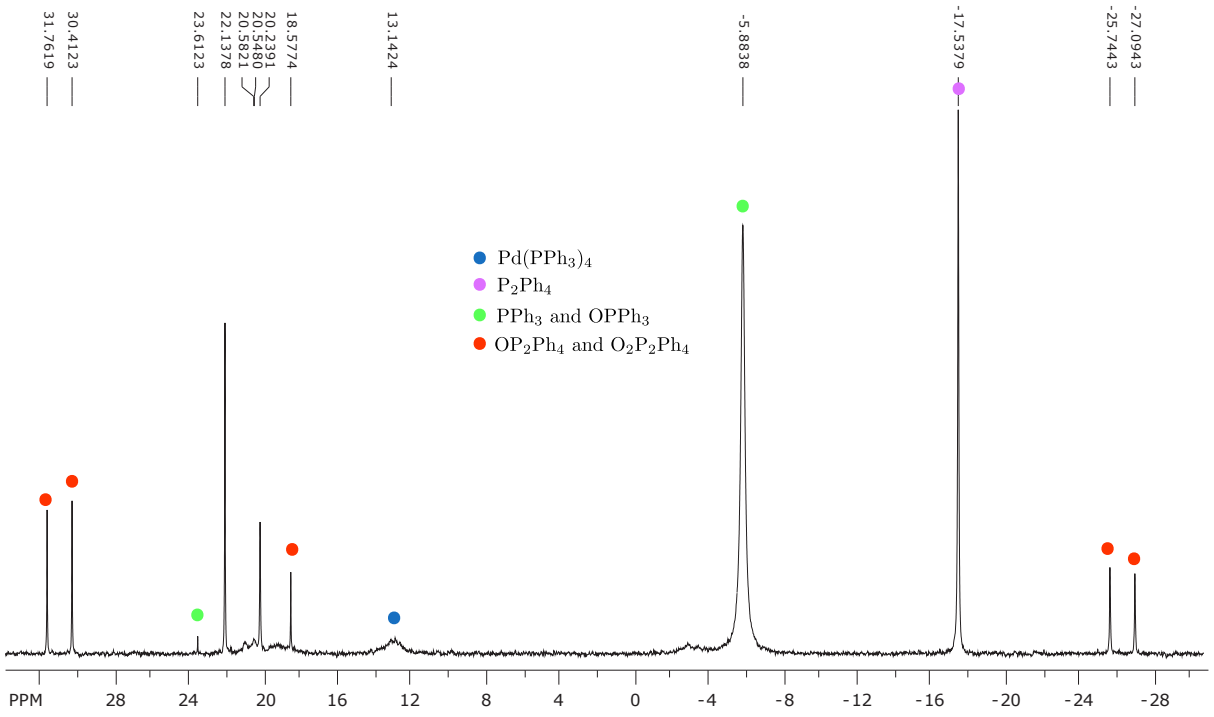

Figure S.23: $^{31}P\{^{1}H\}$ NMR spectrum of the reaction mixture between $Pd(PPh_3)_4$ and P_2Ph_4 after one hour of stirring. Some of the extra resonances were assigned as oxidation products from the presence of OP_2Ph_4 in the P_2Ph_4 batch used. Unambiguous assignments could not be made for the remaining features around +20 ppm.

A suspension of P_2Ph_4 (10 mg, 0.027 mmol, 1.5 equiv) in C_6D_6 (0.5 mL) was added to a pale yellow suspension of $Pt(PPh_3)_4$ (22 mg, 0.018 mmol, 1.0 equiv) in C_6D_6 (0.5 mL) under stirring. During the addition, a slight darkening to orange was observed as well as complete dissolution of the solids. NMR spectra obtained after one hour revealed a large amount P_2Ph_4, but no signals consistent with either free PPh_3 or metallic complexes (Figure S.24). Unreacted $Pt(PPh_3)_4$ could only be observed by ^{1}H NMR spectroscopy, since its ^{31}P NMR signal is very broad at room temperature.[4,6]

S.1.12 Thermal decomposition of solid 3-Ni

A sample of complex **3**-Ni (96 mg, 0.073 mmol) was placed in a sublimator, and brought outside of the box. The sublimator was heated gradually under static vacuum during which the cold finger was loaded with liquid nitrogen to help freeze any volatiles generated during the heating. The aspect of the bright orange solids started to change at around 180 °C, slowly darkening to brown. Meanwhile, white material and a small amounts of oil started depositing on the sides of the flask and on the finger. The temperature was gradually increased to 250 °C over an interval of 40 mins at which point the solids had turned into a fine black powder. After cooling down, the solids were washed with diethyl ether, followed by removal of the volatiles under vacuum from the diethyl ether filtrate. NMR spectroscopy of the generated white residue revealed the presence of only free PPh_3 and diphosphane **1** (in

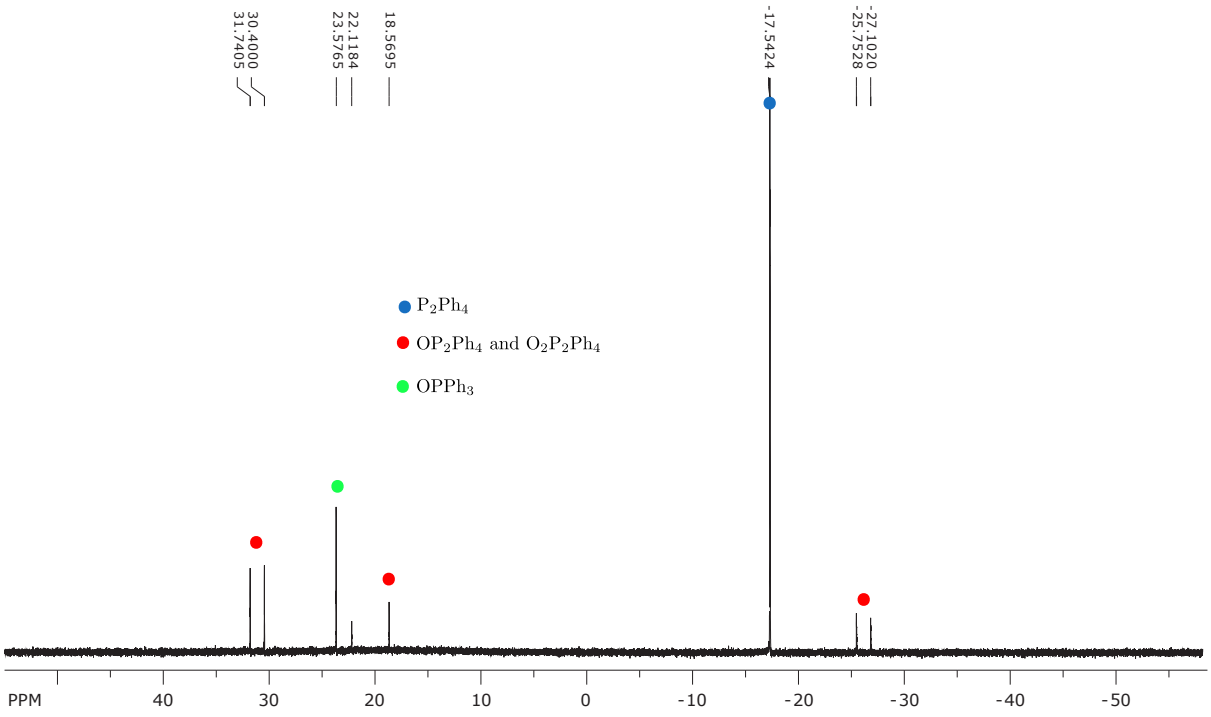

Figure S.24: $^{31}P\{^{1}H\}$ NMR spectrum of the reaction mixture between $Pt(PPh_3)_4$ and P_2Ph_4 after one hour of stirring. The extra resonances were be assigned as oxidation products generated from the presence of OP_2Ph_4 in the P_2Ph_4 batch used.

a ca. 1:1), and a small amount of complex **3**-Ni (Figure S.25). The presence of diphosphane **1** in smaller amounts than a stoichiometric ratio (1.5 times more than PPh_3) is likely the result of it decomposing at above 220 °C.[2]

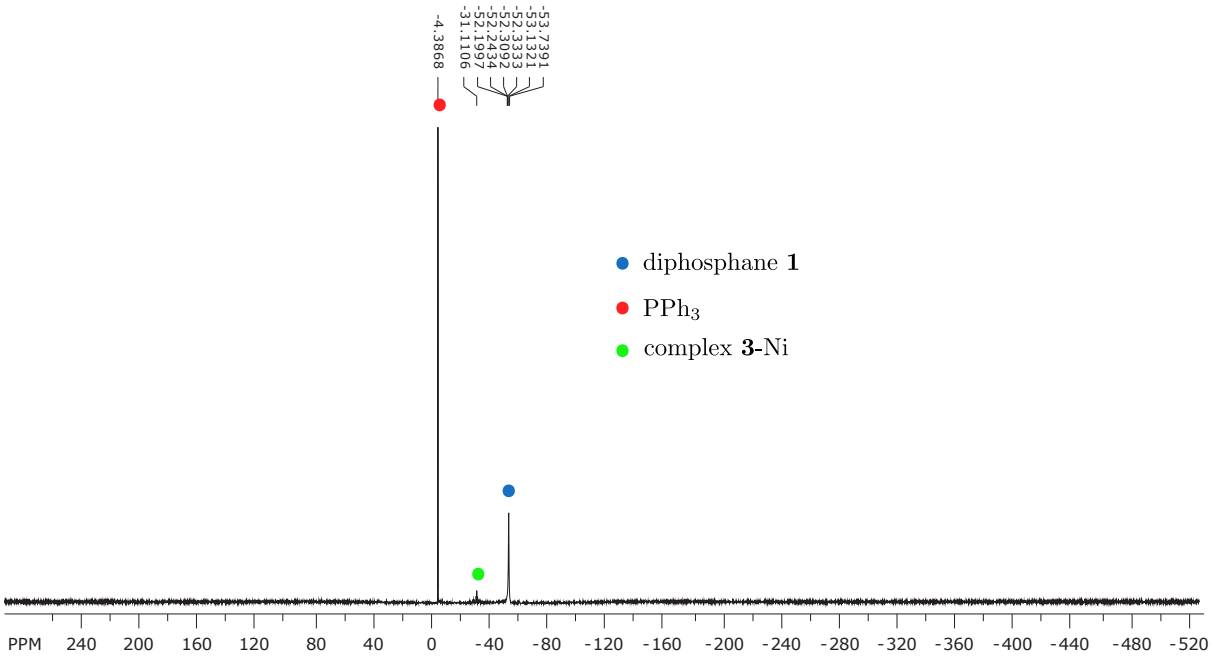

Figure S.25: $^{31}P\{^{1}H\}$ NMR spectrum of the Et_2O filtrate from the thermal decomposition of complex **3**-Ni.

S.2 Crystallographic Details

S.2.1 General X-ray Refinement Methods

Diffraction quality, orange crystals of **2**, **3**-Ni, and **4** were grown directly from crude reaction mixtures in benzene by allowing the homogenous mixtures to sit undisturbed at room temperature. Yellow crystals of **3**-Pd were grown from a toluene solution, to which pentane and tetrahydrofuran (THF) were added prior to storing it at −35 °C. Orange crystals of **3**-Pt were grown from a mixture of toluene and THF that was stored at −35 °C. The crystals were mounted in hydrocarbon oil on a nylon loop or a glass fiber. Low-temperature (100 K) data were collected on a Siemens Platform three-circle diffractometer coupled to a Bruker-AXS Smart Apex CCD detector with graphite-monochromated Mo Kα radiation (λ = 0.71073 Å) for **4**, on a Bruker-AXS X8 Kappa Duo diffractometer coupled to a Smart Apex2 CCD detector with Mo Kα radiation (λ = 0.71073 Å) for **3**-Pt, and on a Bruker D8 three-circle diffractometer coupled to a Bruker-AXS Smart Apex CCD detector with graphite-monochromated Cu Kα radiation (λ = 1.54178 Å) for the other complexes (ϕ- and ω-scans). A semi-empirical absorption correction was applied to the diffraction data using SADABS.[7] The structures were solved by direct methods using SHELXS[8,9] and refined against F^2 on all data by full-matrix least squares with SHELXL-97,[9,10] using established refinement techniques.[11] All non-hydrogen atoms were refined anisotropically. All hydrogen atoms were included in the model at geometrically calculated positions and refined using a riding model. The isotropic displacement parameters of all hydrogen atoms were fixed to 1.2 times the U_{eq} value of the atoms they are linked to (1.5 times for methyl groups). Descriptions of the individual refinements follow below and details of

the data quality and a summary of the residual values of the refinements for all structures are given in the following tables. Further details are provided in the form of *.cif* files available from the CCDC.[12]

S.2.2 Specific X-ray Refinement Details

The compound **2** crystallized in the triclinic space group $P\bar{1}$ with half a molecule of complex and one molecule of pentane per asymmetric unit. The presence of the inversion center in the middle of the Ni–Ni line leads to the three diphosphane **1** bridges to be disordered over two symmetry-imposed positions each, while the two $\{NiPPh_3\}$ fragments were not disordered. The model contains no restraints on either the target molecule and the solvent. A crystallographic summary is provided in Table S.2, while a list of select interatomic distances and angles is provided in Table S.4.

The compounds **3**-Ni and **4** crystallized in the hexagonal space group $R\bar{3}$ with a third of a molecule of complex and two molecules of benzene per asymmetric unit. The model contains no restraints on either the target molecules or the solvents. Crystallographic summaries are provided in Table S.2, while lists of select interatomic distances and angles are provided in Tables S.4 and S.5, respectively.

The compound **3**-Pd crystallized in the triclinic space group $P\bar{1}$ with a whole molecule of complex, one molecule of toluene and one molecule of THF per asymmetric unit. The THF molecule is disordered over two positions. Similarity restraints on 1–2 and 1–3 distances and displacement parameters as well as rigid bond restraints for anisotropic displacement parameters were applied to all atoms in the THF molecules. In addition, similarity restraints were applied to geometrically relate the two THF molecules to one another. The ratio between the two components was refined freely, and the sum of the two occupancies was constrained to unity.[13] The model contains no restraints on either the target molecules or the toluene molecule. A crystallographic summary is provided in Table S.3, while a list of select interatomic distances and angles is provided in Table S.7.

The compound **3**-Pt crystallized in the monoclinic space group *Cc* with one molecule of complex, one toluene, and two THF molecules per asymmetric unit. One phenyl ring of one of the PPh_3 ligands and one of the THF molecules are disordered over two positions. Similarity restraints on 1–2 and 1–3 distances and displacement parameters as well as rigid bond restraints for anisotropic displacement parameters were applied to the three solvent molecules and the disordered phenyl ring. In addition, similarity restraints were applied to geometrically relate the three THF molecules to one another. The ratio between the two components of each disorder was refined freely, and the sum of the two occupancies for each pair was constrained to unity.[13] A crystallographic summary is provided in Table S.3, while a list of select interatomic distances and angles is provided in Table S.8.

The estimated angles between the diphosphane lone pairs listed in Table 1 can be estimated precisely using the formula:

$$\theta' = 180^\circ - 2 \times (180^\circ - \alpha) = 2 \times \alpha - 180^\circ, \text{ where:}$$

$$\alpha = \arccos\left(\frac{\cos(\angle_{\mathrm{P-P-M}})}{\cos(\frac{\angle_{\mathrm{M-P-P-M}}}{2})}\right).$$

This $\alpha = \angle_{\mathrm{P-P-M}}$ when the dihedral angle M–P–P–M is zero and MPPM becomes a planar trapezoid, in which case $\theta' = \theta$ from Table 1. The values for θ and θ' are listed below in Table S.1.

Table S.1: Diphosphane **1** lone pair angle

	θ	θ'
2	45.38	45.48
3-Ni	46.86	46.93
3-Pd	45.42	45.56
3-Pt	47.62	47.64
4	44.12	44.17
Av.	45.88	45.96

S.2.3 X-ray Crystallographic Tables

Table S.2: Crystallographic Data for Nickel Complexes

	2	**3**-Ni	**4**
Reciprocal Net code / CCDC number	D8_10098 / 863743	D8_10112 / 863746	11124 / 863747
Empirical formula, FW (g/mol)	$C_{65}H_{112}Ni_2P_{10}$, 1320.67	$C_{108}H_{126}Ni_2P_8$, 1789.27	$C_{108}H_{126}As_2Ni_2P_6$, 1877.17
Color / Morphology	Orange / Needle	Orange / Block	Orange / Block
Crystal size (mm^3)	$0.50 \times 0.20 \times 0.15$	$0.38 \times 0.16 \times 0.10$	$0.40 \times 0.35 \times 0.30$
Temperature (K)	100(2)	100(2)	100(2)
Wavelength (Å)	1.54178	1.54178	0.71073
Crystal system, Space group	Triclinic, $P\bar{1}$	Hexagonal, $R\bar{3}$	Hexagonal, $R\bar{3}$
Unit cell dimensions (Å, °)	a = 11.3941(2), α = 66.0080(10)	a = 23.0550(2), α = 90	a = 23.0523(8), α = 90
	b = 12.6121(2), β = 82.3230(10)	b = 23.0550(2), β = 90	b = 23.0523(8), β = 90
	c = 14.3410(2), γ = 66.7130(10)	c = 31.0318(4), γ = 120	c = 31.4482(11), γ = 120
Volume ($Å^3$)	1728.51(5)	14284.6(3)	14472.9(9)
Z	1	6	6
Density (calc., g/cm^3)	1.269	1.248	1.292
Absorption coefficient (mm^{-1})	3.138	2.115	1.217
$F(000)$	708	5700	5916
Theta range for data collection (°)	3.37 to 68.24	2.63 to 68.24	1.21 to 30.51
Index ranges	$-13 \le h \le 13$, $-15 \le k \le 15$,	$-27 \le h \le 27$, $-27 \le k \le 27$,	$-32 \le h \le 32$, $-32 \le k \le 32$,
	$-17 \le l \le 17$	$-27 \le l \le 35$	$-44 \le l \le 44$
Reflections collected	34473	95879	135796
Independent reflections, R_{int}	6166 (0.0309)	5155 (0.0379)	9827(0.0357)
Completeness to θ_{max} (%)	97.3	98.9	100.0
Absorption correction	Multi-scan (SADABS)	Multi-scan (SADABS)	Multi-scan (SADABS)
Max. and min. transmission	0.6504 and 0.3030	0.8164 and 0.5004	0.7116 and 0.6417
Refinement method	Full-matrix least-squares on F^2	Full-matrix least-squares on F^2	Full-matrix least-squares on F^2
Data / restraints / parameters	6166 / 0 / 577	5759 / 0 / 359	9827 / 0 / 359
Goodness-of-fit[a]	1.063	1.032	1.028
Final R indices[b] [$I > 2\sigma(I)$]	R_1 = 0.0408, wR_2 = 0.1111	R_1 = 0.0327, wR_2 = 0.0855	R_1 = 0.0277, wR_2 = 0.0695
R indices[b] (all data)	R_1 = 0.0458, wR_2 = 0.1159	R_1 = 0.0376, wR_2 = 0.0905	R_1 = 0.0368, wR_2 = 0.0766
Largest diff. peak and hole ($e \cdot ^{-3}$)	0.848 and −0.224	0.393 and −0.274	0.811 and −0.282

[a] GooF = $\left[\frac{\Sigma[w(F_o^2-F_c^2)^2]}{(n-p)}\right]^{\frac{1}{2}}$ [b] $R_1 = \frac{\Sigma||F_o|-|F_c||}{\Sigma|F_o|}$; $wR_2 = \left[\frac{\Sigma[w(F_o^2-F_c^2)^2}{\Sigma[w(F_o^2)^2]}\right]^{\frac{1}{2}}$; $w = \frac{1}{\sigma^2(F_o^2)+(aP)^2+bP}$; $P = \frac{2F_c^2+\max(F_o^2,0)}{3}$

Table S.3: Crystallographic Data for Palladium and Platinum Complexes

	3-Pd	**3**-Pt
Reciprocal Net code / CCDC number	D8_10132 / 863745	X8_10081 / 863744
Empirical formula, FW (g/mol)	$C_{83}H_{106}OP_8Pd_2$, 1580.24	$C_{87}H_{114}O_2P_8Pt_2$, 1829.72
Color / Morphology	Yellow / Prism	Orange / Block
Crystal size (mm^3)	$0.40 \times 0.30 \times 0.12$	$0.05 \times 0.02 \times 0.01$
Temperature (K)	100(2)	100(2)
Wavelength (Å)	1.54178	0.71073
Crystal system, Space group	Triclinic, $P\bar{1}$	Monoclinic, Cc
Unit cell dimensions (Å, °)	a = 12.3521(3), α = 74.0590(10)	a = 20.4091(11), α = 90
	b = 14.0198(3), β = 80.7290(10)	b = 16.3489(9), β = 111.9700(10)
	c = 23.3487(3), γ = 82.8510(10)	c = 26.2219(18), γ = 90
Volume ($Å^3$)	3823.39(15)	8114.0(8
Z	2	4
Density (calc., g/cm^3)	1.373	1.498
Absorption coefficient (mm^{-1})	5.716	3.649
$F(000)$	1648	3712
Theta range for data collection (°)	1.99 to 68.24	1.65 to 30.51
Index ranges	$-10 \leq h \leq 14$, $-16 \leq k \leq 16$,	$-28 \leq h \leq 29$, $-23 \leq k \leq 23$,
	$-28 \leq l \leq 28$	$-37 \leq l \leq 37$
Reflections collected	73677	105960
Independent reflections, R_{int}	13542 (0.0350)	24728 (0.0580)
Completeness to θ_{max} (%)	100.0	100.0
Absorption correction	Multi-scan (SADABS)	Multi-scan (SADABS)
Max. and min. transmission	0.5471 and 0.2083	0.9644 and 0.8386
Refinement method	Full-matrix least-squares on F^2	Full-matrix least-squares on F^2
Data / restraints / parameters	13542 / 172 / 906	24728 / 469 / 988
Goodness-of-fit[a]	1.264	1.015
Final R indices[b] [$I > 2\sigma(I)$]	R_1 = 0.0539, wR_2 = 0.1587	R_1 = 0.0329, wR_2 = 0.0571
R indices[b] (all data)	R_1 = 0.0594, wR_2 = 0.1624	R_1 = 0.0459, wR_2 = 0.0612
Largest diff. peak and hole ($e \cdot ^{-3}$)	1.960 and −0.859	1.095 and −1.067

[a] GooF = $\left[\frac{\Sigma[w(F_o^2-F_c^2)^2]}{(n-p)}\right]^{\frac{1}{2}}$ [b] $R_1 = \frac{\Sigma||F_o|-|F_c||}{\Sigma|F_o|}$; $wR_2 = \left[\frac{\Sigma[w(F_o^2-F_c^2)^2}{\Sigma[w(F_o^2)^2]}\right]^{\frac{1}{2}}$; $w = \frac{1}{\sigma^2(F_o^2)+(aP)^2+bP}$; $P = \frac{2F_c^2+\max(F_o^2,0)}{3}$

Table S.4: Select interatomic distances [Å] and angles [°] in complex **2**

Ni1–Ni1a	3.9085(5)
P1–P2	2.2239(8)
P3–P4	2.2280(14)
P5–P6	2.2262(14)
P7–P8	2.2241(14)
Ni1–P1	2.1425(6)
Ni1–P3	2.1857(11)
Ni1–P5	2.1811(11)
Ni1–P7	2.0610(11)
Ni1–P4a	2.2412(10)
Ni1–P6a	2.2436(11)
Ni1–P8a	2.1142(11)
Ni1–P1–P2	114.54(3)
Ni1–P3–P4	109.21(5)
Ni1–P5–P6	112.71(5)
Ni1–P7–P8	111.75(5)
P3–P4–Ni1a	115.16(5)
P5–P6–Ni1a	111.82(5)
P7–P8–Ni1a	115.46(5)
P1–Ni1–P3	115.87(3)
P1–Ni1–P5	108.82(3)
P7–Ni1–P1	109.20(3)
P1a–Ni1a–P4	108.86(3)
P1a–Ni1a–P6	115.45(3)
P1a–Ni1a–P8	118.82(3)
P7–Ni1–P5	109.05(4)
P7–Ni1–P3	109.83(4)
P5–Ni1–P3	103.81(4)
P8–Ni1a–P4	105.71(4)
P8–Ni1a–P6	104.98(4)
P4–Ni1a–P6	101.23(4)
P1–Ni1–Ni1a	180
Ni1–Ni1a–P1a	180
P1–Ni1–Ni1a–P1a	180.00(0)
Ni1–P3–P4–Ni1a	7.09(8)
Ni1–P5–P6–Ni1a	5.89(8)
Ni1–P7–P8–Ni1a	9.06(9)
P3–Ni1–P4a	135.09(4)
P5–Ni1–P6a	135.10(4)
P7–Ni1–P8a	131.97(4)
P8a–Ni1–P5	56.69(4)
P8a–Ni1–P3	48.33(4)
P7–Ni1–P4a	56.07(4)
P5–Ni1–P4a	55.84(4)
P7–Ni1–P6a	49.44(4)
P3–Ni1–P6a	63.35(4)

Table S.5: Select interatomic distances [Å] and angles [°] in complex **3**-Ni

Ni1–Ni2	3.9607(6)
P1–P2	2.2274(6)
Ni1–P1	2.1664(4)
Ni1–P1a	2.1664(4)
Ni1–P1b	2.1664(4)
Ni2–P2	2.1790(4)
Ni2–P2a	2.1790(4)
Ni2–P2b	2.1790(4)
Ni1–P3	2.1419(8)
Ni2–P4	2.1637(8)

Ni1–P1–P2	112.74(2)
Ni2–P2–P1	114.11(2)
P3–Ni1–P1	113.001(15)
P3–Ni1–P1a	113.003(15)
P3–Ni1–P1b	113.003(15)
P4–Ni2–P2	114.108(15)
P4–Ni2–P2a	114.109(15)
P4–Ni2–P2b	114.109(15)
P1–Ni1–P1a	105.721(16)
P1–Ni1–P1b	105.722(16)
P1a–Ni1–P1b	105.720(16)
P2–Ni2–P2a	104.463(17)
P2–Ni2–P2b	104.461(17)
P2a–Ni2–P2b	104.461(17)
P3–Ni1–Ni2	180
Ni1–Ni2–P4	180
P3–Ni1–Ni2–P4	0.00(0)
Ni1–P1–P2–Ni2	6.13(4)

Table S.6: Select interatomic distances [Å] and angles [°] in complex **4**

Ni1–Ni2	3.8532(4)
P1–P2	2.2258(4)
Ni1–As1	2.2769(3)
Ni2–As2	2.2492(3)
Ni1–P1b	2.1682(3)
Ni1–P1a	2.1682(3)
Ni1–P1	2.1681(3)
Ni2–P2	2.1519(3)
Ni2–P2b	2.1519(3)
Ni2–P2a	2.1519(3)

Ni1–P1–P2	112.694(17)
Ni2–P2–P1	111.432(17)
P1b–Ni1–P1a	105.995(12)
P1b–Ni1–P1	105.996(12)
P1a–Ni1–P1	105.996(12)
P2–Ni2–P2b	107.287(11)
P2–Ni2–P2a	107.286(11)
P2b–Ni2–P2a	107.288(11)
P1b–Ni1–As1	112.757(10)
P1a–Ni1–As1	112.757(11)
P1–Ni1–As1	112.755(11)
P2–Ni2–As2	111.578(10)
P2b–Ni2–As2	111.575(10)
P2a–Ni2–As2	111.575(10)
As1–Ni1–Ni2	180.0(0)
Ni1–Ni2–As2	180.0(0)
As1–Ni1–Ni2–As2	0.00(±6.60)
Ni1–P1–P2–Ni2	5.38(3)

Table S.7: Select interatomic distances [Å] and angles [°] in complex **3**-Pd

Pd1–Pd2	4.0577(6)
Pd1–P1	2.3505(16)
Pd1–P3	2.3562(15)
Pd1–P5	2.3638(15)
Pd2–P2	2.3555(15)
Pd2–P4	2.3473(15)
Pd2–P6	2.3350(16)
Pd1–P7	2.2941(15)
Pd2–P8	2.2930(16)
P1–P2	2.222(2)
P3–P4	2.228(2)
P5–P6	2.223(2)

P7–Pd1–P1	111.35(6)
P7–Pd1–P3	117.85(5)
P7–Pd1–P5	109.41(6)
P8–Pd2–P2	110.40(6)
P8–Pd2–P4	112.40(6)
P8–Pd2–P6	117.04(6)
P1–Pd1–P3	102.41(6)
P1–Pd1–P5	106.63(5)
P3–Pd1–P5	108.49(5)
P6–Pd2–P4	105.03(6)
P6–Pd2–P2	106.60(5)
P4–Pd2–P2	104.43(5)
P2–P1–Pd1	110.15(7)
P1–P2–Pd2	115.13(8)
P4–P3–Pd1	111.88(7)
P3–P4–Pd2	113.88(7)
P6–P5–Pd1	113.99(8)
P5–P6–Pd2	111.24(7)
Pd1–P1–P2–Pd2	11.8(1)
Pd1–P3–P4–Pd2	2.3(1)
Pd1–P5–P6–Pd2	12.6(1)

Table S.8: Select interatomic distances [Å] and angles [°] in complex **3**-Pt

Pt1–Pt2	4.0846(3)
Pt1–P1	2.2969(10)
Pt1–P2	2.3061(10)
Pt1–P3	2.3067(11)
Pt2–P4	2.3016(11)
Pt2–P6	2.3023(10)
Pt2–P5	2.3074(10)
P1–P4	2.2219(15)
P2–P5	2.2222(15)
P3–P6	2.2204(15)
Pt1–P7	2.2656(11)
Pt2–P8	2.2531(11)

P7–Pt1–P1	117.07(4)
P7–Pt1–P2	114.29(4)
P7–Pt1–P3	110.58(4)
P8–Pt2–P4	114.00(4)
P8–Pt2–P6	113.81(4)
P8–Pt2–P5	113.41(4)
P1–Pt1–P2	104.34(4)
P1–Pt1–P3	104.94(4)
P2–Pt1–P3	104.46(4)
P4–Pt2–P6	106.30(4)
P4–Pt2–P5	104.19(4)
P6–Pt2–P5	104.14(4)
P4–P1–Pt1	113.58(5)
P1–P4–Pt2	114.10(5)
P5–P2–Pt1	114.69(5)
P2–P5–Pt2	112.86(5)
P6–P3–Pt1	113.96(5)
P3–P6–Pt2	113.74(5)
P7–Pt1–Pt2	176.11(3)
Pt1–Pt2–P8	179.87(3)
Pt1–P1–P4–Pt2	5.09(8)
Pt1–P2–P5–Pt2	3.94(8)
Pt1–P3–P6–Pt2	1.48(8)

References

[1] G. R. Fulmer, A. J. M. Miller, N. H. Sherden, H. E. Gottlieb, A. Nudelman, B. M. Stoltz, J. E. Bercaw and K. I. Goldberg, *Organometallics*, 2010, **29**, 2176–2179.

[2] D. Tofan and C. C. Cummins, *Angew. Chem., Int. Ed.*, 2010, **49**, 7516–7518.

[3] J. Langer, H. Görls, G. Gillies and D. Walther, *Z. Anorg. Allg. Chem.*, 2005, **631**, 2719–2726.

[4] C. A. Tolman, W. C. Seidel and D. H. Gerlach, *J. Am. Chem. Soc.*, 1972, **94**, 2669–2676.

[5] D. R. Coulson, L. C. Satek and S. O. Grim, in *Inorganic Syntheses*, ed. R. J. Angelici, John Wiley & Sons, Inc., 2007, vol. 28, pp. 107–109.

[6] R. Ugo, F. Cariati, G. L. Monica and J. J. Mrowca, in *Inorganic Syntheses*, ed. R. J. Angelici, John Wiley & Sons, Inc., 2007, vol. 28, pp. 123–126.

[7] G. M. Sheldrick, SHELXTL*; Bruker AXS, Inc.: Madison, WI (USA), 2005–2011.*

[8] G. M. Sheldrick, *Acta Crystallogr., Sect. A: Fundam. Crystallogr.*, 1990, **46**, 467–473.

[9] G. M. Sheldrick, *Acta Crystallogr. A*, 2008, **64**, 112–122.

[10] G. M. Sheldrick, SHELXL-97: Program for crystal structure determination*; University of Göttingen, 1997.*

[11] P. Müller, *Crystallogr. Rev.*, 2009, **15**, 57–83.

[12] *These data can be obtained free of charge from The Cambridge Crystallographic Data Centre via http://www.ccdc.cam.ac.uk/data_request/cif under the Cambridge Structural Database deposition numbers 863743–863747*.

[13] P. Müller, R. Herbst-Irmer, A. L. Spek, T. R. Schneider and M. R. Sawaya, *Crystal Structure Refinement: A Crystallographer's Guide to SHELXL*, IUCr Texts on Crystallography; Oxford University Press: Oxford, 2006.